iJOIN

INFSO-ICT-317941

INFSO-ICT-317941 iJOIN

IR 2.1

Preliminary report on state-of-the-art and iJOIN PHY requirements, and scenarios

Editor:	Atta Quddus, UNIS
Deliverable nature:	Confidential
Suggested readers:	iJOIN GA
Due date:	April 30th, 2013
Delivery date:	April 30th, 2013
Version:	1.0
Total number of pages:	71
Reviewed by:	GA members
Keywords:	iJOIN
Resources consumed	24,4 PM

Abstract

This report presents an overview of the activities carried out by the work package 2 (WP2) during the first six months of the project. These activities include providing state-of-art physical layer channel models and performance indicators. Moreover, preliminary analysis of the state-of-art radio access techniques and backhauling methods is also provided. In order to meet the challenges of an small cell deployment with a holistic design of radio access network and backhaul network promising candidate technologies for the physical layer are introduced. Based on these technologies a consolidated list of assumptions is derived which serves as input to WP5.

List of authors

Company	Author
IMC	Umer Salim (umer.salim@intel.com)
TUD	Jens Bartelt (jens.bartelt@ifn.et.tu-dresden.de)
UoB	Dirk Wübben (wuebben@ant.uni-bremen.de)
	Henning Paul (paul@ant.uni-bremen.de)
	Guang Xu (xu@ant.uni-bremen.de)
UNIS	Omer Waqar (o.waqar@surrey.ac.uk)
	Atta Quddus (a.quddus@surrey.ac.uk)
	Muhammad Ali Imran (m.imran@surrey.ac.uk)
CEA	Valentin Savin (valentin.savin@cea.fr)
SCBB	Massinissa Lalam (massinissa.lalam@sagemcom.com)
TI	Boldi Mauro Renato (mauro.boldi@telecomitalia.it)
	Bruno Melis (bruno1.melis@telecomitalia.it)

History

Modified by	Date	Version	Comments
Atta Quddus	30.04.2013	1.0	Final version IR2.1 report

Table of Contents

List of authors ... 2
History ... 3
Table of Contents ... 4
List of Figures ... 6
List of Tables ... 7
Abbreviations ... 8
1 Introduction ... 11
2 Executive Summary ... 13
3 State of the art ... 15
3.1 PHY State of the art of 3GPP LTE Rel. 10/11/12 ... 15
3.1.1 General Architecture ... 15
3.1.2 PHY Layer Parameters ... 16
3.1.2.1 Frame Type ... 16
3.1.2.2 Uplink Overview ... 18
3.1.2.3 Downlink Overview ... 22
3.1.3 Channel Models ... 25
3.1.3.1 Point-to-Point Channel Models ... 25
3.1.3.2 Cooperative Channel Models ... 30
3.1.4 Key Performance Indicators ... 33
3.2 PHY State of the art for Radio Access ... 36
3.2.1 Distributed and iterative multiuser detection ... 36
3.2.2 Inter-Cell Interference Coordination (ICIC) and Coordinated Multi-Point Transmission (CoMP) 37
3.2.3 Joint network-channel coding ... 38
3.2.4 Frequency-domain RoF ... 39
3.3 PHY State of the art for Backhauling ... 40
3.3.1 Fibre-based backhauling ... 40
3.3.2 Wireless and mmWave backhauling ... 40
3.3.3 In-band backhauling ... 42
4 PHY Candidate Technologies ... 44
4.1 iJOIN Entities ... 45
4.1.1 RAN as a Service (RANaaS) ... 45
4.1.2 iJOIN Small Cell (iSC) ... 45
4.1.3 Virtual eNB ... 45
4.1.4 iJOIN Network Controller (iNC) ... 45
4.1.5 iJOIN Local Gateway (iLGW) ... 45
4.1.6 iJOIN Transport Node (iTN) ... 46
4.1.7 J1/J2 interfaces ... 46
4.2 CT 2.1: In-network processing ... 46
4.2.1 Scenario description ... 46
4.2.2 Assumptions ... 46
4.2.3 Technology requirements ... 47
4.2.4 iJOIN objectives addressed ... 48
4.3 CT 2.2: Multipoint turbo detection ... 48
4.3.1 Scenario description ... 48
4.3.2 Assumptions ... 48
4.3.3 Technology requirements ... 49
4.3.4 iJOIN objectives addressed ... 50
4.4 CT 2.3: Joint network-channel coding ... 50
4.4.1 Scenario description ... 50
4.4.2 Assumptions ... 51
4.4.3 Technology requirements ... 51
4.4.4 iJOIN objectives addressed ... 52
4.5 CT 2.4: Sum-Rate and Energy-Efficiency metrics of DL COMP with backhaul constraints ... 52
4.5.1 Scenario description ... 52

4.5.2 Assumptions ... 53
4.5.3 Technology requirements ... 53
4.5.4 iJOIN objectives addressed ... 54
4.6 CT 2.5: Cloud Based Joint-Processing and Partially Centralized Inter-Cell Interference Coordination ... 54
4.6.1 Scenario description ... 54
4.6.2 Assumptions ... 55
4.6.3 Technology requirements ... 56
4.6.4 iJOIN objectives addressed ... 56
4.7 CT2.6: Data compression over RoF ... 56
4.7.1 Scenario description ... 56
4.7.2 Assumptions ... 59
4.7.3 Technology requirements ... 60
4.7.4 iJOIN objectives addressed ... 60
4.8 CT2.7: 60GHz backhauling ... 60
4.8.1 Scenario description ... 60
4.8.2 Assumptions ... 61
4.8.3 Technology requirements ... 61
4.8.4 iJOIN objectives addressed ... 62
5 Consolidated WP2 Assumptions ... 63
5.1 Architectural and technology deployment assumptions ... 63
5.2 WP2 Implementation assumptions ... 63
6 Summary and Conclusion ... 65
Acknowledgements and Disclaimer ... 66
References ... 67

List of Figures

Figure 3-1: Overview of the general architecture of 3GPP LTE [7] 15
Figure 3-2: Frame structure Type 1 (FDD) [74] 17
Figure 3-3: Frame structure Type 2 (TDD) [74] 17
Figure 3-4: Uplink resource grid [74] 19
Figure 3-5: SC-FDMA principle [81] 19
Figure 3-6: PUCCH/PUSCH allocation area (PRACH areas given as an example) 20
Figure 3-7: Mapping to physical resource blocks for PUCCH [74] 20
Figure 3-8: Rate 1/3 tail biting convolutional encoder [74] 21
Figure 3-9: Rate 1/3 turbo encoder (dotted lines apply for trellis termination only) [74] 21
Figure 3-10: Overview of uplink physical channel processing [74] 21
Figure 3-11: Cumulative distribution function of the cell/user throughput 35
Figure 3-12: Example of a multiple access relay channel (MARC) 39
Figure 4-1: Preliminary draft of the iJOIN Architecture 45
Figure 4-2: A UE is served by several iSCs, cooperating through In-Network-Processing 46
Figure 4-3: Multipoint turbo detection investigation context 48
Figure 4-4: Proposed scenario for joint network channel coding. 50
Figure 4-5: Joint Network Channel coding for the MARC 51
Figure 4-6: A three cell network with limited backhaul capacities of J1 links (centralized architecture). 52
Figure 4-7: Each iSC is connected with each other through J2 interfaces (de-centralized architecture). 53
Figure 4-8: An exemplary scenario showing joint transmission and interference coordination. 55
Figure 4-9: Conventional RoF architecture 57
Figure 4-10: Frequency Domain RoF architecture: transmitter part 59
Figure 4-11: Frequency Domain RoF architecture: receiver part 59
Figure 4-12: Scenario for 60 GHz backhauling 61

List of Tables

Table 3-1: Uplink-downlink configurations [74] 18
Table 3-2: Modulation schemes 23
Table 3-3: Transmission Modes in LTE 24
Table 3-4: Precoding for 2 antennas 24
Table 3-5: Delay profiles for E-UTRA channel models [2] 25
Table 3-6: Extended Pedestrian A model (EPA) [2] 25
Table 3-7: Extended Vehicular A model (EVA) [2] 26
Table 3-8: Extended Typical Urban model (ETU) [2] 26
Table 3-9: Channel model parameters [2] 26
Table 3-10: Spatial correlation matrices [2] 27
Table 3-11: Correlation Values [2] 27
Table 3-12: MIMO correlation matrices for high correlation [2] 28
Table 3-13: MIMO correlation matrices for medium correlation [2] 29
Table 3-14: MIMO correlation matrices for low correlation [2] 29
Table 3-15: Baseline channel parameters for outdoor macrocell deployments 30
Table 3-16: Application Scenarios for LTE-Advanced Relays [8] 30
Table 3-17: Baseline parameters for fixed outdoor relay deployment in dense urban (case 1) [4] 31
Table 3-18: Delay spread, angle spread parameters for RN-UE and eNB-RN links [12] 33
Table 3-19: ITU minimum requirements in terms of spectrum efficiency [3] 34
Table 3-20: Performance of DL CS/CB-CoMP 4 x 2 (antenna configuration C) (UMi, FDD) [4] 34
Table 3-21: Performance of DL JP-CoMP 4 x 2 (antenna configuration C) (UMi, FDD) [4] 35
Table 3-22: Performance of UL CoMP 2 x 4 (antenna configuration A) (UMi, FDD) [4] 35
Table 3-23: Key performance indicator at PHY level 36
Table 3-24: Overview over wireless backhaul technologies 41
Table 3-25: Link Budget for 28 and 72 GHz frequencies [79] 42
Table 3-26: Relay Types in 3GPP LTE Rel.10 43
Table 4-1: List of iJOIN PHY Candidate Technologies (CTs) 44
Table 4-2: Mapping of PHY CTs to iJOIN Common Scenarios (CS) 44
Table 4-3: Assumptions of CT2.1: In-network processing 47
Table 4-4: Requirements of CT2.1: In-network processing 47
Table 4-5: Assumptions of CT2.2: Multipoint turbo detection 49
Table 4-6: Requirements of CT2.2: Multipoint turbo detection 49
Table 4-7: Assumptions of CT2.3: Joint network channel coding 51
Table 4-8: Requirements of CT2.3: Joint network channel coding 51
Table 4-9: Assumptions of CT2.4: Sum-rate and Energy efficiency metrics of DL-COMP 53
Table 4-10: Requirements of CT2.4: Sum-rate and Energy efficiency metrics of DL-COMP 54
Table 4-11: Assumptions of CT2.5: Cloud based Joint processing and partially centralised ICIC 55
Table 4-12: Requirements of CT2.5: Cloud based Joint processing and partially centralised ICIC 56
Table 4-13: Categorization of non-ideal backhaul [6] 58
Table 4-14: Assumptions of CT2.6: Data compression over RoF 59
Table 4-15: Requirements of CT2.6: Date compression over RoF 60
Table 4-16: Assumptions of CT2.7: 60 GHz backhauling 61
Table 4-17: Requirements of CT2.7: 60 GHz backhauling 61
Table 5-1: Architectural and deployment assumptions per Candidate Technology 63
Table 5-2: Implementation Assumptions per Candidate Technology 64

Abbreviations

3GPP	3rd Generation Partnership Program
AoA	Angle of Arrival
AoD	Angle of Departure
AF	Amplify-and-Forward
ASA	Angle Spread of Arrival
ASD	Angle Spread of Departure
ARQ	Automatic Repeat Request
BH	Backhaul
BD	Block Diagonalization
bps	Bits per Second
BS	Base Station
CB	Coordinated Beamforming
CDD	Cyclic Delay Diversity
CDF	Cumulative Distribution Function
CoMP	Coordinated Multi-Point Transmission
CPRI	Common Public Radio Interface
CRC	Cyclic Redundancy Check
CF	Carrier Frequency
CS	iJOIN Common Scenario
CSI	Channel State Information
CT	Candidate Technology
DAS	Distributed Antenna System
DCI	Downlink Control Information
DF	Decode-and-Forward
DMRS	Demodulation Reference Signal
DPC	Dirty Paper Coding
DS	Delay Spread
DSL	Digital Subscriber Line
DwPTS	Downlink Pilot Time Slot
eNB	Evolved Node B
EPC	Evolved Packet Core
EPDCCH	Enhanced Physical Downlink Control Channel
E-UTRAN	Evolved Universal Terrestrial Radio Access Network
EPA	Extended Pedestrian A (channel model)
ETU	Extended Typical Urban (channel model)
EVA	Extended Vehicular A (channel model)
FD	Frequency Domain
FD-RoF	Frequency Domain Radio over Fibre
FDD	Frequency Division Duplex
FEC	Forward Error Correction
FFT	Fast Fourier Transform
FSO	Free Space Optics
GSM	Global System for Mobile Communications
GP	Guard Period
HARQ	Hybrid Automatic Repeat Request
HSS	Home Subscriber Service
ICI	Inter-Cell Interference
ICIC	Inter- Cell Interference Coordination
IFFT	Inverse Fast Fourier Transform
iJOIN	Interworking and JOINt Design of an Open Access and Backhaul Network Architecture for Small Cells based on Cloud Networks
IP	Internet Protocol
iSC	iJOIN Small Cell
JNCC	Joint Network Channel Coding

KPI	Key Performance Indicator
LLR	Log Likelihood Ratio
LDPC	Low Density Parity Check
LOS	Line of Sight
LTE	Long Term Evolution
LTE-A	Long Term Evolution-Advanced
MAC	Medium Access Control
MARC	Multiple Access Relay Channel
MBMS	Multimedia Broadcast and Multicast Services
MCS	Modulation and Coding Schemes
MIMO	Multiple-Input Multiple Output
MME	Mobility Management Entity
MUD	Multi-User Detection
NC	Network Coding
NLOS	Non Line of Sight
OBSAI	Open Base Station Architecture Initiative
OFDM	Orthogonal Frequency Division Multiplexing
OFDMA	Orthogonal Frequency Division Multiple Access
ORI	Open Radio Interface
PAPR	Peak-to-Average Power Ratio
PBCH	Physical Broadcast Channel
PCFICH	Physical Control Format Indicator Channel
PCRF	Policy Control and Charging Function
PDCCH	Physical Downlink Control Channel
PDSCH	Physical Downlink Shared Channel
PDU	Payload Data Unit
P-GW	Package Gateway
PHICH	Physical Hybrid ARQ Indicator Channel
PHY	Physical Layer
PL	Path Loss
PMCH	Physical Multicast Channel
PRACH	Physical Random Access Channel
PUCCH	Physical Uplink Control Channel
PUSCH	Physical Uplink Shared Channel
QAM	Quadrature Amplitude Modulation
QoS	Quality of Service
QPSK	Quadrature Phase Shift Keying
RAN	Radio Access Network
RANaaS	RAN-as-a-service
RAP	Radio Access Point
RAT	Radio Access Technology
RB	Resource Block
RF	Radio Frequency
RIT	Radio Interface Technology
RLC	Radio Link Control
RMA	Rural Macro (channel model)
RN	Relay Node
RoF	Radio over Fibre
RRC	Radio Resource Control
RRH	Remote Radio Head
RRM	Radio Resource Management
SC	Small Cell
SCM	Spatial Channel Model
SC-FDMA	Single-Carrier Frequency Division Multiple Access
S-GW	Service Gateway
SF	Shadow Fading
SINR	Signal to Interference and Noise Ratio

SNR	Signal to Noise Ratio
SotA	State-of-the-Art
SRS	Sounding Reference Signal
TB	Transport Block
TBS	Transport Block Size
TDD	Time Division Duplex
TTI	Transmission Time Interval
TrCH	Transport Channel
UE	User Equipment
UMa	Urban Macro (channel model)
UMi	Urban Micro (channel model)
UpPTS	Uplink Pilot Time Slot
W-CDMA	Wideband Code Division Multiple Access
WLAN	Wireless Local Area Network
WP	Work Package
ZF	Zero Forcing

1 Introduction

Due to the increasing popularity of iPhones, netbooks, tablets, and other smart phones, the mobile data traffic has experienced an unprecedented growth. Furthermore, it is expected that this traffic will be increased by 500 to 1000 times by 2020 [1]. In order to meet this exponential increase in throughput requirement, dense deployment of small cells and (partly) centralized processing of RAN (radio access network) functionalities are two promising strategies being investigated in the iJOIN project.

The reason to complement cellular networks with small cell deployment is twofold: Firstly, the distance between the small cell (SC) and user equipment (UE) decreases and thus path-loss is reduced exponentially. Hence maintaining the same Quality of Service (QoS), modulation order can be increased and redundancy added by forwards error correcting (FEC) codes can be decreased which results in significant gain in data rate. Secondly, small cells facilitate better use of spectrum as compared to large cells (e.g., macro cells) and consequently result in large data rate. Some other advantages of small cell deployment include the reduction in coverage holes, increased energy efficiency, and improved cost efficiency. However, the main challenge of small cell deployment is the strong inter-cell interference (ICI) in both uplink and the downlink, which requires appropriate processing techniques. Without such techniques, e.g., the potential of multiple-input-multiple-output (MIMO) of increasing date rate linearly with the minimum of transmit and receive antennas cannot be realized in the presence of high interference. Hence, the ICI is a main challenge in the deployment of small cells. On the other hand, as a UE is likely to be in the vicinity of several SCs, a joint processing among these SCs can significantly improve the system performance. Within this project we introduce the iJOIN small cell (iSC) and the RAN-as-a-service (RANaaS) concept, which allows for a flexible cooperative processing among iSCs and a (partly) centralized processing in the RANaaS. As communication between these entities is provided by the backhaul network, both the radio access and the backhaul have to be optimized jointly in order to maximize the overall system performance. In iJOIN project, J1 terminology is used to represent the backhaul links between RANaaS and iSCs. Furthermore, backhaul links that connect iSCs together are represented by J2.

The main objective of WP2 in iJOIN is to investigate Physical layer (PHY) approaches for a joint design of access and backhaul network with the aim of increasing the overall throughput, energy efficiency, and utilisation efficiency of very dense small networks with (partly) centralized processing. Motivated by this fact, in this report, the preliminary state-of-the-art (SotA) for physical layer techniques for ICI reduction and different approaches for joint transmit and receive processing are presented. Furthermore, in order to implement these techniques in a distributed system, backhaul interfaces are required either between the iSCs or between iSCs and RANaaS. State of the art channel models and related PHY parameters are also required to study and analyse the performance indicators.

Based on the SotA analysis, promising candidate technologies (CTs) for the physical layer are introduced, which are topics of further investigations within the iJOIN project. In the future, these approaches will be we studied for the four iJOIN common scenarios (CSs) which have been developed in WP5. The detailed description of these CSs is given in IR5.1 and a brief description is given below:

CS1 Stadium: This scenario represents a stadium which is full of people who are gathered for a special match. Most of the people want to capture these special moments and share with their friends through internet instantly. Some of them want to listen to the commentary and views of the experts using You-tube. Due to this huge mobile data traffic, there is a risk of poor cellular service or even completely lose connectivity. The potential solution for this problem is to deploy iSCs which increase the network capacity and QoS.

CS2 Square: This is about an area which is usually surrounded by shops, offices, restaurants, and parks. In general this square area exists in almost every university campus. Thousands of people visit this place for social activities. In order to provide good quality broadband services, the network capacity and coverage have to be increased through dense deployment of iSCs.

CS3 Wide-area continuous coverage: This scenario represents a city centre in which thousands of users use broadband services during busy hours. This area usually covers several kilometres and surrounded by large buildings and shopping plazas (i.e., dense urban area). Dense small cells are employed to increase the coverage and total network capacity.

CS4 Airport/Shopping Mall: This represents an indoor scenario in general which includes airport and shopping malls as special cases. At airport, thousands of people use internet while waiting for the plane and similarly at shopping malls, broadband services are used by many people at a time. iSCs are employed at the airports and shopping malls to accommodate this huge data traffic.

After the executive summary in section two, the 3GPP LTE network will be introduced in section three. The SotA channel models are then presented for point-to-point MIMO (without cooperation) and cooperative (which usually include relays) systems. In this section, various performance metrics are also described which are used to compare the different CTs. Furthermore, in order to achieve the iJOIN objectives, different SotA PHY techniques for the access network are described. A comprehensive literature survey about the backhaul schemes is also given at the end of this section.

In the fourth section, various CTs from PHY perspective are presented where each candidate technology is applicable for at-least one iJOIN common scenario. Furthermore, the assumptions and requirements for each CT are also explicitly defined. The iJOIN objectives achieved by each CT are also discussed.

Finally, the fifth section is devoted to the consolidated assumptions and requirements i.e., it gives a holistic overview of the assumptions and requirements of all the CTs. This section facilitates to derive the iJOIN architecture and set the basis for the other WPs.

2 Executive Summary

This report describes the main activities carried out by WP2 during the first six months of the project. The main objective of this report is to present state of the art literature survey for the PHY layer techniques, which have the potential to reduce (or even exploit) inter-cell interference in the downlink and exploit multi-user diversity in the uplink with joint processing and joint detection. Furthermore, a state of the art literature on current backhauling of cellular networks and emerging new trends is also provided. This consequently results in significant improvement of the various performance metrics (which are also discussed in this report), particularly for the cell-edge users in the realistic cellular environment. The report is organized as follows:

In Section 3, the SotA channel models, PHY parameters, performance indicators, RAN and backhauling techniques are presented. A general architecture of a 3GPP LTE network is defined in section 3.1.1. It is discussed that the entire network is divided into E-UTRAN (evolved universal terrestrial radio access network) and the EPC (evolved packet core). E-UTRAN is responsible for transmission between the UEs whereas EPC is mainly used for control, management, and interworking with outside networks. The description about small cells, relays, and remote radio heads (RRHs) is also provided in this section. The SotA PHY layer parameters are described in section 3.1.2. It is discussed that LTE operates in both frequency division duplexing (FDD) and time division duplexing (TDD). The description about different PHY channels and signals for both uplink and downlink is provided. Moreover, the modulation and coding schemes which are used in SotA LTE are also mentioned. The brief description about the SotA MIMO architecture and about its different transmission modes is also provided. The channel models for point-to-point networks (i.e., without cooperation) are given in section 3.1.3.1. In this section, 3GPP channel delay profiles, maximum Doppler frequencies and correlation matrices (that represents correlation between iSCs and UEs) are given. Moreover, path-loss model for an outdoor scenario is also given in this section. The SotA channel models for cooperative systems (e.g., when a relay is present) are presented in section 3.1.3.2. In this section, scenarios are defined in which relays can be beneficial. Moreover, the models and/or values are given for large-scale fading, angle of departure, angle of arrivals, delay spread, and cross-correlation (e.g., correlation in shadowing may exist between different relay to iSC links).

Key performance indicators (which will later be used to compare different PHY techniques) are discussed in section 3.1.4. The SotA study for the cell-spectral efficiency and cell edge-user spectral efficiency of different coordinated multipoint transmission (CoMP) schemes is given. The SotA requirements and iJOIN objectives for different performance metrics are explicitly defined in this section.

Section 3.2 is about the SotA PHY techniques being applicable to small cell deployments. In section 3.2.1, the idea of distributed and iterative multi-user detection (e.g., using turbo principle) is presented. Moreover, it is discussed that the trade-off exists between the detection ability and amount of exchange information (i.e., quantisation level). The idea of CoMP is discussed in section 3.2.2 and it is mentioned that benefits of traditional MIMO can be realized for cellular networks by mitigating or exploiting inter-cell interference. A comprehensive SotA literature survey is given for different types of CoMP. Since backhaul and channel state information (CSI) on the transmit side are the main challenges for practical CoMP, different schemes are discussed in this section to reduce this backhauling and other signalling overheads. In section 3.2.2, the main advantages of CoMP are also listed. The promising technique of joint network channel coding (e.g., distributed Turbo and LDPC codes) is discussed in section 2.2.3 in the context of multiple relay access channel i.e., when a single relay is used for the uplink transmission of many UEs simultaneously. The SotA literature on this particular topic is also presented. It is discussed that through joint network channel coding, network's capacity can be increased considerably. Another new approach known as Radio over Fibre (RoF) is discussed in section 3.2.4 and the standardization works in this field are also provided.

The SotA backhaul techniques are presented in section 3.3. Fibre-based backhauling is discussed in section 3.3.1 and previous literature survey related to this topic is also presented. It is discussed in section 3.3.2 that wireless backhaul is easier to deploy and has many other advantages over wired backhaul. Moreover, wireless backhaul can be categorized into traditional microwave (5-42 GHz), sub 6 GHz microwave, unlicensed (60 GHz) and licensed (70-80 GHz) millimetre wave systems, and Free-space optics systems. The main characteristics, advantages and limitations of each type of wireless backhaul are also discussed in this section. Furthermore, the link budget analysis is also presented for microwave and millimetre wave backhauls under different cases. In-band backhauling is explained in section 3.3.3. Furthermore, depending upon the mode of carrier frequency, duplex operation and cell-ID, various types of relays are discussed in this section.

Furthermore, in Section 4, seven PHY CTs are discussed, which address one or more of the four iJOIN CSs that have been developed in WP5. Moreover, the explicit assumptions, requirements, and objectives of each CT 2.x are explicitly defined. The CT 2.1 “In-network processing” is described in section 4.2 performs partly distributed multiuser detection by exchanging local estimates between iSCs. In section 4.3, the CT 2.2 “Multipoint turbo detection” is presented which implements the iterative turbo detection in a distributed fashion. In section 4.4, joint network-channel coding is described as a promising CT to increase the spectral efficiency of uplink access network. In this CT, the network code at the relay and channel codes at the UEs are jointly optimized to achieve the iJOIN objectives. With the aim to increase the spectral efficiency (or sum-rate) and energy efficiency, downlink (DL) CoMP with backhaul constraints is presented as a CT 2.4 in section 4.5. Similar to section 4.5, inter-cell interference coordination is considered in section 4.6 as CT 2.5. CT 2.6 describes the RoF architecture in detail in section 4.7. First the conventional RoF architecture is described and then novel frequency-domain RoF architecture is proposed in order to increase the area throughput and energy efficiency considering the non-ideal backhaul links. The preliminary and brief discussion for the CT 2.7 (60GHz backhauling) is provided in section 4.8. It is mentioned that the 60GHz wireless link is used as a backhaul between the small cell and RANaaS whereas the LTE access link between UE and the small cell. The main objective of this scenario is to increase the throughput by optimizing the functional split.

Finally, the WP2 assumptions and requirements for all CTs in the consolidated form are presented in the Section 5. The assumptions are categorized as 1) Architectural assumptions and 2) Implementation assumptions.

3 State of the art

3.1 PHY State of the art of 3GPP LTE Rel. 10/11/12

The physical layer of 3GPP LTE-A is based on orthogonal frequency division multiple access (OFDMA). It is a wideband system that avoids fixed frequency planning like in GSM (global system for mobile communications) and is more flexible than W-CDMA (wideband code division multiple access) systems. While true orthogonal frequency division multiplexing (OFDM) is only used in the downlink, most of its components are reused in the uplink, which uses single-carrier FDMA (SC-FDMA).

LTE was designed to be as flexible as possible, supporting a large number of different modulation schemes, code and data rates, carriers, bandwidths, MIMO techniques, and TDD as well as FDD. Resources can be flexibly assigned to users and the transmission scheme is adapted to the momentary channel gain. As the name LTE indicates, it also offers room for improvement in the future.

3.1.1 General Architecture

An overview of the general architecture of a 3GPP LTE network is depicted in Figure 3-1. It can be separated into the E-UTRAN and the EPC [26]. While the E-UTRAN is responsible for the direct radio connection to users, the EPC handles the communication with other networks as well as most of the management.

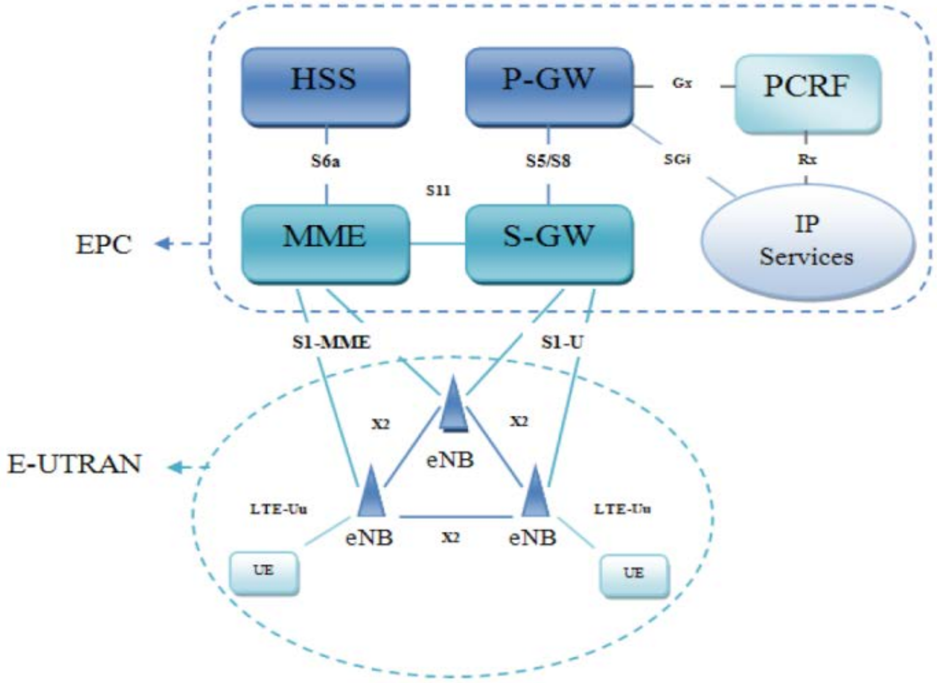

Figure 3-1: Overview of the general architecture of 3GPP LTE [7]

The UEs send their data to and receive transmissions from the base stations denoted eNB (evolved node B), who are in turn connected to the EPC. An eNB controls multiple UEs and is responsible for radio resource management (RRM) and control, MAC, and PHY.

The communication with other IP services is managed via the S-GW (service gateway) and the P-GW (package gateway). While the S-GW acts as a router and mobility anchor, the P-GW allocates IP addresses, enforces QoS, and filters packets accordingly.

The MME is the central control node of the network. It manages bearers and connections as well as some security aspects. A data base of all subscriber information is located at the HSS (home subscriber service). Charging and QoS are controlled by the PCRF (policy control and charging function).

All elements are connected using different interfaces. Most important of these are the S1 and X2 interfaces that connect an eNB to the EPC and other eNBs, respectively, and the radio interface between the UEs and an eNB, which is called Uu.

The 3GPP EPS architecture is designed under the assumption that logical network entities correspond to physical entities, and that logical network functions are located in such physical network entities. To provide an example, the logical network entity "eNB" corresponds to a physical entity in the network, i.e. a base station. The logical function "RRM" is executed in this eNB, therefore also in a specific physical location. The separation of logical and physical network entities and functions as such is therefore not addressed specifically in the 3GPP specifications.

In the current access topology macrocell base stations (BSs) with directional antennas are used for mid-scale to large-scale coverage whereas microcell BSs equipped with omnidirectional antennas typically cover distances of about 100 m [28]. The future trend to smaller cells is reflected by recent research and development of picocells and femtocells. Small cells are low power cells aimed at covering a restricted geographical area, offloading the macrocell network of users that are generally in bad conditions (indoor) or in dense environments (e.g., airport, shopping mall, train station). Two types of cells that are usually associated to the small cell terminology can be identified:

a) picocells usually cover small but dense areas (hot-spot) such as mall, airport, etc,

b) femtocells are usually located in residential or corporate environments (mainly indoor oriented)

Except some technical discrepancies obviously reflected by the type of the cell (in terms of raw computational power, simultaneously supported users, covered area, etc.) the main difference lies in the way the cells are deployed and connected to the operator's core network. Indeed, if picocells are usually operator-deployed, thus part of the operator's network planning, femtocells are end-user deployed and usually make use of the user's broadband access (DSL line or cable) as a third-party backhaul. Picocells support the exact same set of functionalities and feature as macrocells in the 3GPP view. However, femtocells have some limitations due to the unplanned nature of their deployment and their possible high density resulting in mutual interference.

A further trend that can be observed in the later releases of 3GPP is the deployment of small cells that do not offer the same functionality as macro BS, but only work in support of them:

1. **Relays** [26]: In contrast to traditional repeaters that just amplify and re-broadcast a signal, the 3GPP relays demodulate and decode received data and then re-transmit it. They thereby enhance the signals quality. Relays can be either used to increase the network density or extend the coverage. In contrast to macro BS they do not require a direct backhaul link, since this is provided by the donor BS. 3GPP has defined a few categories / types of relays, these are described in Section 3.3.3.
2. **Remote Radio Heads (RRHs)** [27]: A RRH can be seen a part of a widely distributed antenna system. It usually consists of an antenna and transceiver, but little data processing devices. Like the relay, it re-transmits the received signal to a donor BS, e.g. via a fibre connection, but without decoding the data. It can be used to increase coverage or signal quality as well, but it also opens the possibility to combine the signals of multiple RRHs for a joint detection at the donor BS.

3.1.2 PHY Layer Parameters

The LTE physical layer is described in the 3GPP technical specifications TS 36.211 for the physical channel [74] and TS 36.212 for the modulation and coding scheme (MCS) [80]. This section will briefly present the main physical layer parameters in LTE. For more details, the reader should refer to the previously mentioned specifications.

3.1.2.1 Frame Type

LTE can operate in both FDD and TDD modes allowing its deployment in paired and unpaired spectrum. Both modes share the same underlying framework: radio access schemes, subframe formats, configuration protocols, system architecture, procedures, etc.

Two 10 ms radio frame types are introduced for transmission in LTE:

- **Type 1 applicable to FDD**: uplink and downlink frames are simultaneously transmitted on different frequencies. This type can be applied to both half and full duplex systems, i.e., systems where reception and emission could be done at the same time (full) or not (half). A frame structure type 1 consists of 20 slots of length T_{slot} = 0.5 ms, numbered from 0 to 19. One subframe i is made of the two consecutive slots 2i and $2i$ +1. The minimum resource in time domain is one subframe. Figure

3-2 shows the type 1 frame structure. In this figure, T_s is the basic time unit corresponding to the sampling frequency of 30.72 MHz.

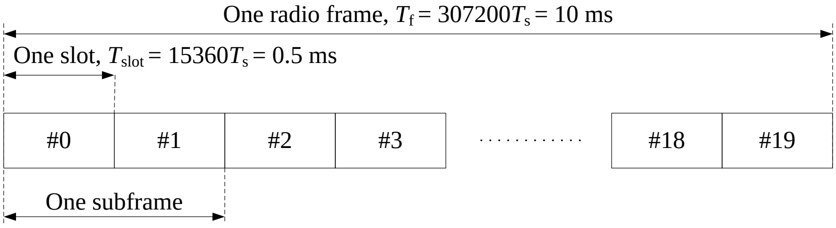

Figure 3-2: Frame structure Type 1 (FDD) [74]

- **Type 2 applicable to TDD**: uplink and downlink frames are alternatively transmitted on the same frequency. A 10 ms frame structure type 2 is made of two half-frames of length 5 ms each. Each half-frame consists of five subframes of length 1 ms. As for frame structure type 1, each subframe i is defined as two slots, $2i$ and $2i+1$ of length T_{slot} =0.5ms. The schematic is visualized in Figure 3-3.

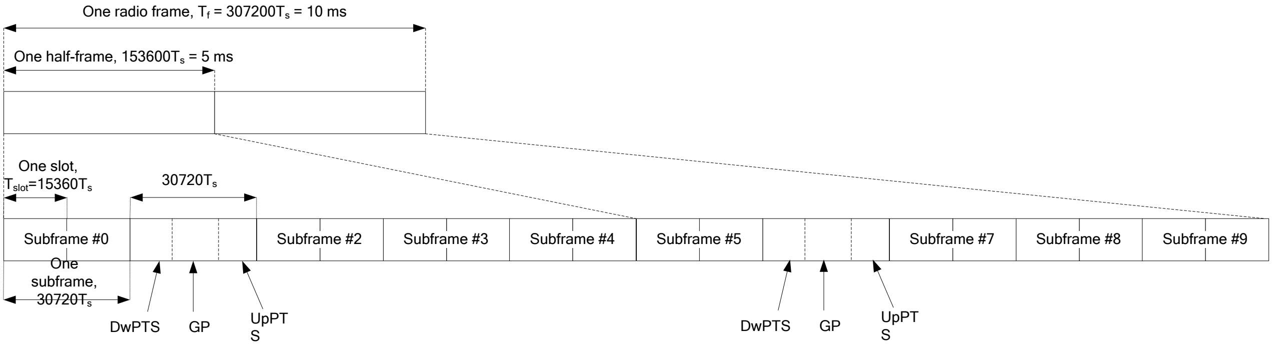

Figure 3-3: Frame structure Type 2 (TDD) [74]

The uplink-downlink configurations are presented in Table 3-1, where each subframe in a radio frame can either be noted “D” for downlink transmissions, “U” for uplink transmissions or “S” for a special subframe with the three following fields illustrated in Figure 3-3.

- DwPTS (downlink pilot time slot)
- GP (guard period)
- UpPTS (uplink pilot time slot)

Table 3-1: Uplink-downlink configurations [74]

Uplink-downlink configuration	Downlink-to-Uplink Switch-point periodicity	Subframe number									
		0	**1**	**2**	**3**	**4**	**5**	**6**	**7**	**8**	**9**
0	5 ms	D	S	U	U	U	D	S	U	U	U
1	5 ms	D	S	U	U	D	D	S	U	U	D
2	5 ms	D	S	U	D	D	D	S	U	D	D
3	10 ms	D	S	U	U	U	D	D	D	D	D
4	10 ms	D	S	U	U	D	D	D	D	D	D
5	10 ms	D	S	U	D	D	D	D	D	D	D
6	5 ms	D	S	U	U	U	D	S	U	U	D

3.1.2.2 Uplink Overview

3.1.2.2.1 Physical Channels/Signals

In uplink, the physical layer is divided into physical channels. Channels are separated in two groups depending on the type of information they transport:

- **Physical Channels**: The physical channels carry information from the higher layers. Three types of physical channels are defined in uplink:
    - *Physical Uplink Control Channel* (PUCCH): dedicated channel of one user to carry uplink control information (such as reporting, acknowledgment …).
    - *Physical Uplink Shared Channel* (PUSCH): shared space among the users to carry data information and/or reporting (if PUCCH does not suffice).
    - *Physical Random Access Channel* (PRACH): used by users to trigger a random access if needed.
- **Physical Signals**: The physical signals do not carry information from the higher layers. Two types of physical signals are defined in uplink
    - *Demodulation Reference Signal* (DMRS): used within a PUCCH or PUSCH transmission to help the base station in demodulating the data.
    - *Sounding Reference Signal* (SRS): used for uplink scheduling purpose among a set of users.

3.1.2.2.2 Resource Allocation

Uplink resources are allocated per subframe, where a subframe is made of two consecutive slots. One slot is structured in a time-frequency grid as shown in Figure 3-4. Subcarriers are grouped to form a Resource Block (RB), which represents the smallest allocation unit. Usually subcarriers are 15 kHz spaced and 12 subcarriers form one RB. The total number of RBs n_{PRB} for the frequency domain depends on the system bandwidth (e.g., 50 RBs for a 10 MHz system, 100 RBs for a 20 MHz system …).

To limit Peak-to-Average Power Ratio (PAPR) issue, Single-Carrier Frequency Division Multiple Access (SC-FDMA) is used in the time domain. The idea is to assign collocated frequency resources (subcarriers) to one user when scheduled as shown by Figure 3-5. The number of SC-FDMA symbols used in the time domain of the grid depends if extended cyclic prefix is enabled (6 symbols) or not (7 symbols).

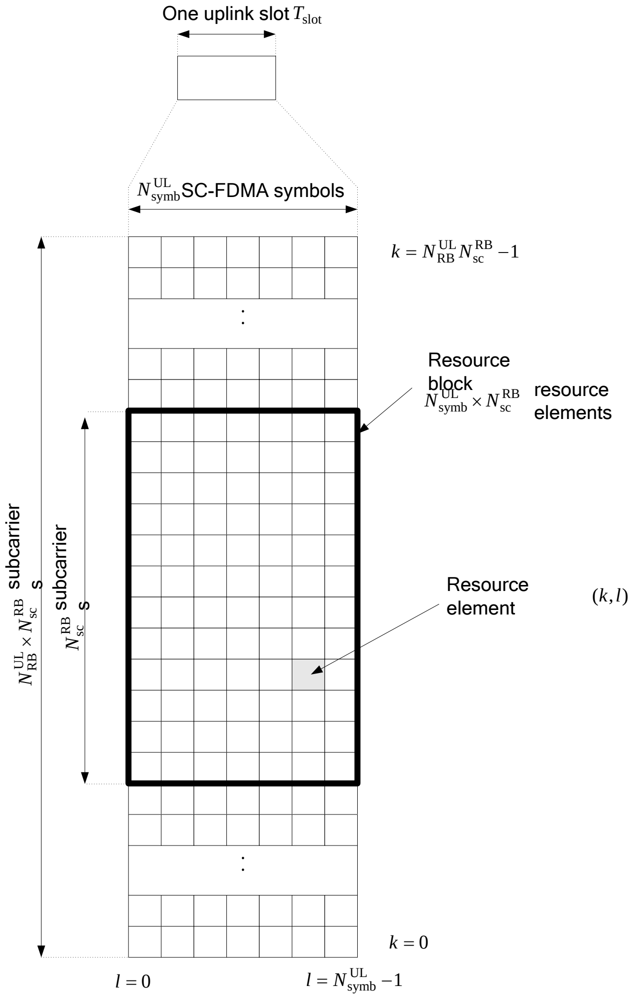

Figure 3-4: Uplink resource grid [74]

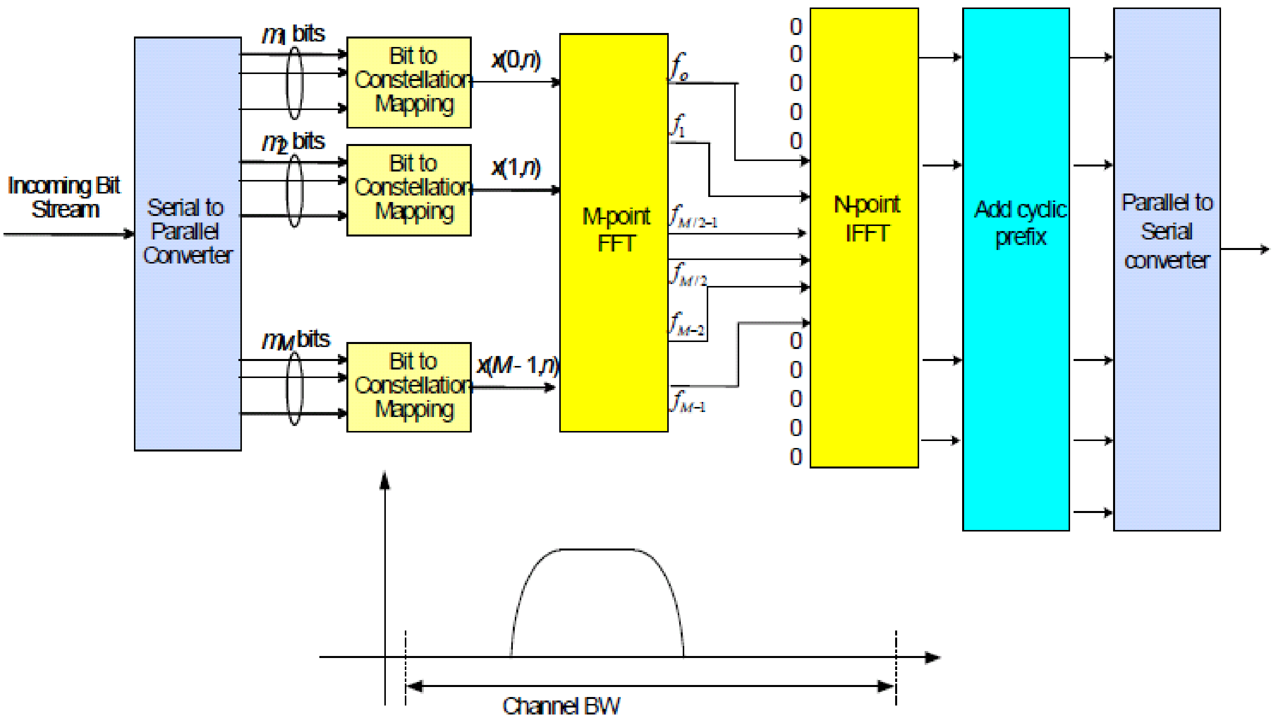

Figure 3-5: SC-FDMA principle [81]

Both extremities of the spectrum are dedicated to PUCCH transmission, while the spectrum centre is the PUSCH area. Regarding the PRACH, this channel is 6 RBs long and made of subcarriers with a lower spacing, 1.25 kHz instead of 15 kHz. Its exact place in one frame (FDD) or in an uplink occasion within one frame (TDD) is governed by Table 5.7.1-2 and Table 5.7.1-3 of [74], respectively. An example is shown in Figure 3-6.

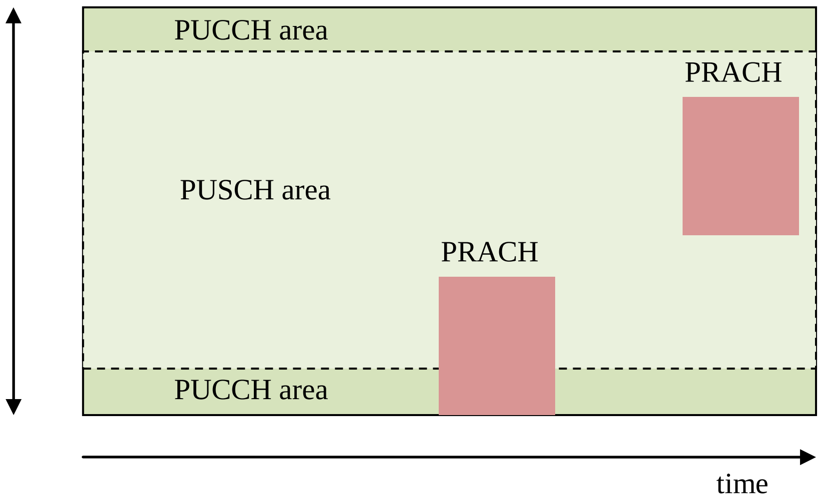

Figure 3-6: PUCCH/PUSCH allocation area (PRACH areas given as an example)

To increase diversity, frequency hopping is introduced for the PUCCH/PUSCH allocation. On a slot basis, the frequency allocation is moved in a mirror fashion for PUCCH as shown in Figure 3-7 for 4 PUCCHs.

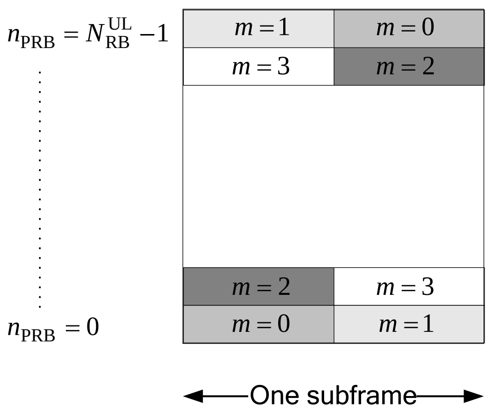

Figure 3-7: Mapping to physical resource blocks for PUCCH [74]

For PUSCH, optional frequency hopping can be defined on slot/subframe basis with a mirror or a “random” pattern. Exact details on the mapping of the channels and the signals to the resource element of the grids within a frame can be found in [74].

3.1.2.2.3 Modulation and Coding Scheme

Uplink data transmission supports QPSK, 16QAM, and 64QAM modulation. The bit-to-symbol mapping is given in section 7 of [74]. Channel coding is made either by a rate 1/3 binary convolutional code (shown in Figure 3-8) or a rate 1/3 turbo code (shown in Figure 3-9), while rate matching allows coding rate flexibility [80]. More details can be found in [80] for each physical channel/signal encoding, including CRC attachment, channel encoder choice, and code block segmentation/concatenation.

In terms of useful data allocation, the downlink control information (DCI) used by the base station to specify the uplink MCS to be used by the mobile contains (but not only) the resources allocated in terms of RB and the TBS in case of a new transmission (which depends on the number of spatial layers in case of MIMO).

Based on the presence or not of a SRS, the last SC-FDMA symbol of a subframe (made of 14 OFDM symbols with normal prefix) is either occupied or free, As DMRS signals are always transmitted on the 4th SC-FDMA symbols of one slot (i.e. 2 DMRS signals per subframe), a resource block will be made of 11 or 12 SC-FDMA symbols, each one made of 12 subcarriers. Once the number of available symbols is derived from the previous operations, the data stream made of TBS bits is encoded with a rate 1/3 channel encoder and rate matching will select the corresponding number of bits to fill the grid of SC-FDMA symbols allocated to data.

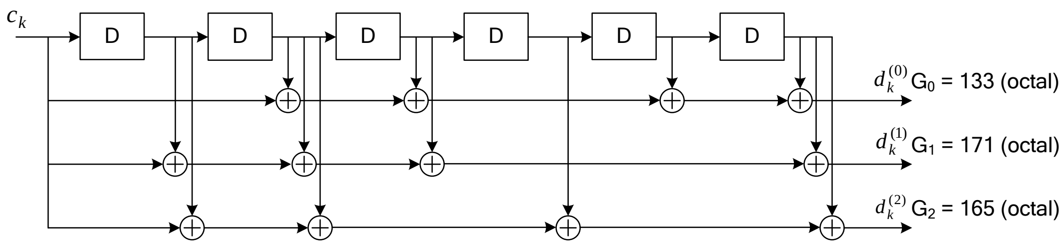

Figure 3-8: Rate 1/3 tail biting convolutional encoder [74]

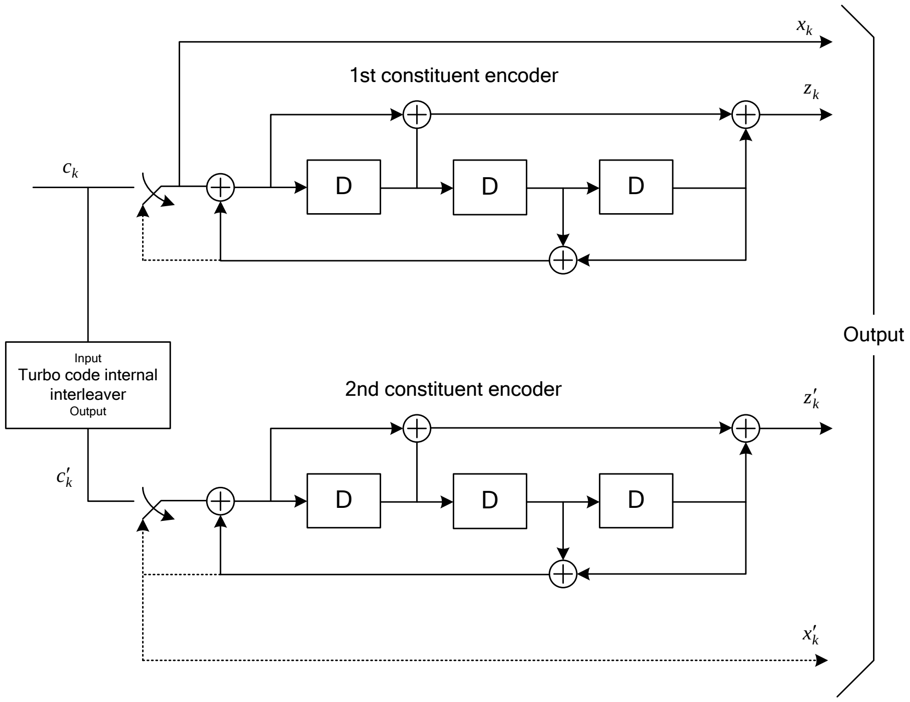

Figure 3-9: Rate 1/3 turbo encoder (dotted lines apply for trellis termination only) [74]

3.1.2.2.4 MIMO

Spatial multiplexing is also supported in the uplink (starting from Release 10) with a maximum of 4 transmit antennas. A maximum of two codewords (resulting from the channel encoding) can be transmitted. Those codewords are mapped into υ layers, which represent the maximum number of spatial streams the BS can detect. A precoding matrix is then applied to distribute the layers over the transmit antennas. Details of the procedure and the precoding matrices are given in [74]. It should be noted that space-time block coding is not supported in the LTE uplink.

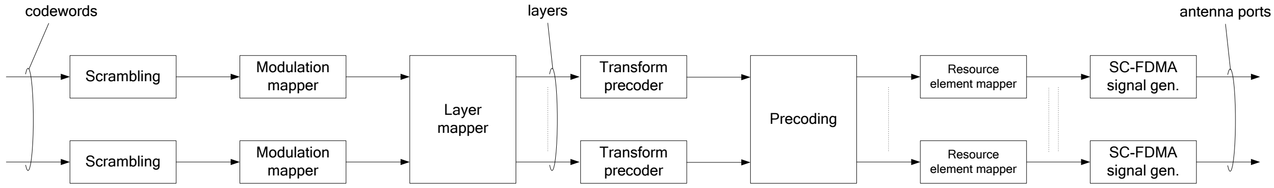

Figure 3-10: Overview of uplink physical channel processing [74]

3.1.2.3 Downlink Overview

3.1.2.3.1 Physical Channels/Signals

The smallest time-frequency unit for downlink transmission is defined as a resource element. It is one OFDM subcarrier for the duration of one OFDM symbol. The available time-frequency resources are categorized in terms of these resource elements which can be flexibly assigned to users as per the application requirements, users' demands, and scheduling guidelines. An LTE resource block is composed by 12 OFDM subcarriers transmitted for the duration of one LTE slot, which has a length of 0.5 ms. To allow coherent demodulation of data by users, some resource elements in each resource block serve as reference signals for learning the channel state.

A downlink physical channel corresponds to a set of resource elements carrying information originating from higher layers. Channels are separated in two groups depending on the type of information they transport:

- **Physical Channels**: The physical channels carry information from the higher layers. The physical channels defined for downlink are:
    - *Physical Broadcast Channel* (PBCH): This physical channel carries system information for UEs requiring to access the network.
    - *Physical Control Format Indicator Channel* (PCFICH): As the name implies the PCFICH informs the UE about the format of the signal being received. It indicates the number of OFDM symbols used for the PDCCHs, whether 1, 2, or 3.
    - *Physical Downlink Control Channel* (PDCCH): The main purpose of this physical channel is to carry mainly scheduling information of different types:
        - Downlink resource scheduling
        - Uplink power control instructions
        - Uplink resource grant
        - Indication for paging or system information

      The PDCCH contains a message known as the Downlink Control Information (DCI) which carries the control information for a particular UE or group of UEs.
    - *Physical Downlink Shared Channel* (PDSCH): The PDSCH is the main data bearing channel which is allocated to users on a dynamic and opportunistic basis. The PDSCH carries data in what's known as Transport Blocks (TB) which correspond to a MAC payload data unit (PDU). They are passed from the MAC layer to the PHY layer once per Transmission Time Interval (TTI).
    - *Physical Hybrid ARQ Indicator Channel* (PHICH): This channel is used to report the hybrid automatic repeat request (HARQ) status. It carries the HARQ ACK/NACK signal indicating whether a transport block has been correctly received. The HARQ indicator is 1 bit long - "0" indicates ACK, and "1" indicates NACK.
    - *Physical Multicast Channel* (PMCH): This channel defines the physical layer structure to carry Multimedia Broadcast and Multicast Services (MBMS). The PMCH is designed for a single-frequency network and it requires that the base stations transmit with tight time synchronization the same modulated symbols.
    - *Enhanced Physical Downlink Control Channel* (EPDCCH): This control channel carries scheduling assignments. An enhanced physical downlink control channel is transmitted using an aggregation of one or several consecutive enhanced control channel elements where each former element consists of multiple enhanced resource element groups.
- **Physical Signals**: A downlink physical signal corresponds to a set of resource elements used by the physical layer but does not carry information originating from higher layers. The following downlink physical signals are defined:
    - *Reference Signals*: The basic purpose of reference signals is to help the users in estimating the channel impulse response. Reference signals are generated as the product of an

orthogonal sequence and a pseudo-random numerical sequence. A specified reference signal is assigned to each cell within a network and acts as a cell-specific identifier. When the eNB has more than one antenna, the reference signals are transmitted so that users can estimate impulse response associated with each transmitting antenna.

- *Synchronization Signals*: Synchronization signals use special type of pseudo-random orthogonal sequences. These are classified as primary and secondary synchronization signals, depending how they are used by UE during the cell search procedure. Both primary and secondary synchronization signals are transmitted regularly by the cells so as to enable users search and camp on appropriate cell.

3.1.2.3.2 Modulation and Coding Scheme

3GPP defines two types of channel coding schemes which can be applied to transport channels (TrCHs):

- tail biting convolutional coding
- turbo coding.

The details for these coding schemes have been provided above in the uplink overview for coding schemes in Section 3.1.2.2.3.

Concerning the downlink modulation schemes, the bits which are obtained at the output of the coding function are converted to the symbols using the selected modulation scheme. This operation transforms the bit streams in appropriate number of complex valued modulated symbol streams [74]. The modulation schemes which can be used are given in Table 3-2.

Table 3-2: Modulation schemes

Physical channel	Modulation schemes
PDSCH	QPSK, 16QAM, 64QAM
PMCH	QPSK, 16QAM, 64QAM

3.1.2.3.3 Transmission modes and Spatial Multiplexing (MIMO) in LTE Downlink

In the downlink, LTE uses technologies such as MIMO to achieve high data rates; however, it also offers fallback technologies such as transmit diversity or SISO. Beamforming is also supported. However, in this case the number of base station antennas is not specified; it depends on the implementation.

All UEs are configured with a transmission mode to help them determine how to process data transmissions received on the PDSCH. The transmission modes actually indicate specifically the mode for PDSCH transmissions identified in the PDCCH. The transmission mode configured for an individual UE is determined by both the capability of the UE and also the capabilities and engineering of the eNB cell site. The mode chosen indicates the subset of downlink transmission schemes that will be used for this UE. While the UE maintains an active connection, the eNB will decide which downlink antenna transmission scheme to use based on feedback received from the UE. Transmission modes also influence or limit the types of channel quality feedback reports that the UE needs to generate and send back to the network. Table 3-3 defines the transmission modes which were standardized in Release 11.

Table 3-3: Transmission Modes in LTE

Transmission Modes in LTE		
Transmission Mode	**Description**	**Comment**
1	Single transmit antenna	single antenna port; port 0
2	Transmit diversity	2 or 4 antennas
3	Open loop spatial multiplexing with cyclic delay diversity (CDD)	2 or 4 antennas
4	Closed loop spatial multiplexing	2 or 4 antennas
5	Multi-user MIMO	2 or 4 antennas
6	Closed loop spatial multiplexing using a single transmission layer	1 layer (rank 1), 2 or 4 antennas
7	Beamforming	single antenna port, port 5 (virtual antenna port, actual antenna configuration depends on implementation)
8	Dual-layer beamforming	dual-layer transmission, antenna ports 7 and 8
9	Multi-layer beamforming	Up to 8 layers , antenna ports 7 to 14
10	Multi-layer beamforming	Up to 8 layers , antenna ports 7 to 14

In LTE, one or two code words are mapped to one to four layers. To achieve multiplexing, a precoding is carried out. In this process, the layers are multiplied by a precoding matrix from a defined code book and distributed to the various antennas. This precoding is known to both the transmitter and the receiver. In the specification, code books are defined for one, two, and four antennas, as well as for spatial multiplexing (with and without cyclic delay diversity (CDD)) and transmit diversity. Table 3-4 shows the code book for spatial multiplexing with two antennas as an example. Code books for four antennas are also defined [74].

Table 3-4: Precoding for 2 antennas

Codebook index	**Number of layers** υ	
	1	**2**
0	$\frac{1}{\sqrt{2}}\begin{bmatrix}1\\1\end{bmatrix}$	$\frac{1}{\sqrt{2}}\begin{bmatrix}1 & 0\\0 & 1\end{bmatrix}$
1	$\frac{1}{\sqrt{2}}\begin{bmatrix}1\\-1\end{bmatrix}$	$\frac{1}{2}\begin{bmatrix}1 & 1\\1 & -1\end{bmatrix}$
2	$\frac{1}{\sqrt{2}}\begin{bmatrix}1\\j\end{bmatrix}$	$\frac{1}{2}\begin{bmatrix}1 & 1\\j & -j\end{bmatrix}$
3	$\frac{1}{\sqrt{2}}\begin{bmatrix}1\\-j\end{bmatrix}$	-

3.1.3 Channel Models

3.1.3.1 Point-to-Point Channel Models

Point to point channel models typically apply to the case where there is no cooperation involved via intermediate relay nodes. Furthermore, classically the variations (commonly known as fading) of a wireless channel are classified as either *large-scale* or *small-scale*. Large-scale fading consists of two processes: a *mean path loss* due to a decrease in the strength of the signal as a function of the increasing distance from the transmitter and log-normally distributed variations about the mean (also called *shadowing*). Small-scale fading (or multipath fading) occurs due to constructive and destructive combination of radio waves arriving at the receiver through multiple reflective paths and is the main focus of this section. The multipath propagation channels typically consist of:

- A delay profile in the form of a "tapped delay-line", characterized by a number of taps at fixed positions on a sampling grid. The profile can be further characterized by the root mean square (r.m.s.) delay spread (DS) and the maximum delay spanned by the taps.
- A combination of channel model parameters that include the Delay profile and the Doppler spectrum that is characterized by a classical spectrum shape and a maximum Doppler frequency.
- A set of correlation matrices defining the correlation between the UE and eNB antennas in case of multi-antenna systems.

3GPP has defined following channel models for E-UTRA work [2].

3.1.3.1.1 3GPP Channel Delay Profiles

These delay profiles are selected to be representative of low, medium and high delay spread environments. The resulting model parameters are defined in Table 3-5 and the tapped delay line models are defined in Table 3-6, Table 3-7 and Table 3-8, respectively.

Table 3-5: Delay profiles for E-UTRA channel models [2]

Model	Number of channel taps	Delay spread (r.m.s.)	Maximum excess tap delay (span)
Extended Pedestrian A (EPA)	7	45 ns	410 ns
Extended Vehicular A (EVA)	9	357 ns	2510 ns
Extended Typical Urban (ETU)	9	991 ns	5000 ns

Table 3-6: Extended Pedestrian A model (EPA) [2]

Excess tap delay [ns]	Relative power [dB]
0	0.0
30	-1.0
70	-2.0
90	-3.0
110	-8.0
190	-17.2
410	-20.8

Table 3-7: Extended Vehicular A model (EVA) [2]

Excess tap delay [ns]	Relative power [dB]
0	0.0
30	-1.5
150	-1.4
310	-3.6
370	-0.6
710	-9.1
1090	-7.0
1730	-12.0
2510	-16.9

Table 3-8: Extended Typical Urban model (ETU) [2]

Excess tap delay [ns]	Relative power [dB]
0	-1.0
50	-1.0
120	-1.0
200	0.0
230	0.0
500	0.0
1600	-3.0
2300	-5.0
5000	-7.0

3.1.3.1.2 Combination of Channel Model Parameters

Table 3-9 shows propagation conditions that are used for the performance measurements in multi-path fading environment for low, medium and high Doppler frequencies.

Table 3-9: Channel model parameters [2]

Model	Maximum Doppler frequency
EPA 5Hz	5 Hz
EVA 5Hz	5 Hz
EVA 70Hz	70 Hz
ETU 30Hz	30 Hz
ETU 70Hz	70 Hz
ETU 300Hz	300 Hz

3.1.3.1.3 MIMO Channel Correlation Matrices

The MIMO channel correlation matrices defined in this section apply for the antenna configuration (of transmit antennas nT x number of receive antennas nR) using uniform linear arrays at both eNB and UE. Table 3-10 defines the channel spatial correlation matrix R_{spat} , where the parameters α and β denote the spatial correlation between the antennas at the eNB and UE.

Table 3-10: Spatial correlation matrices [2]

Antenna configuration	Spatial correlation matrix
1x2	$R_{spat} = R_{UE} = \begin{bmatrix} 1 & \beta \\ \beta^* & 1 \end{bmatrix}$
2x2	$R_{spat} = R_{eNB} \otimes R_{UE} = \begin{bmatrix} 1 & \alpha \\ \alpha^* & 1 \end{bmatrix} \otimes \begin{bmatrix} 1 & \beta \\ \beta^* & 1 \end{bmatrix} = \begin{bmatrix} 1 & \beta & \alpha & \alpha\beta \\ \beta^* & 1 & \alpha\beta^* & \alpha \\ \alpha^* & \alpha^*\beta & 1 & \beta \\ \alpha^*\beta^* & \alpha^* & \beta^* & 1 \end{bmatrix}$
4x2	$R_{spat} = R_{eNB} \otimes R_{UE} = \begin{bmatrix} 1 & \alpha^{1/9} & \alpha^{4/9} & \alpha \\ \alpha^{1/9^*} & 1 & \alpha^{1/9} & \alpha^{4/9} \\ \alpha^{4/9^*} & \alpha^{1/9^*} & 1 & \alpha^{1/9} \\ \alpha^* & \alpha^{4/9^*} & \alpha^{1/9^*} & 1 \end{bmatrix} \otimes \begin{bmatrix} 1 & \beta \\ \beta^* & 1 \end{bmatrix}$
4x4	$R_{spat} = R_{eNB} \otimes R_{UE} = \begin{bmatrix} 1 & \alpha^{1/9} & \alpha^{4/9} & \alpha \\ \alpha^{1/9^*} & 1 & \alpha^{1/9} & \alpha^{4/9} \\ \alpha^{4/9^*} & \alpha^{1/9^*} & 1 & \alpha^{1/9} \\ \alpha^* & \alpha^{4/9^*} & \alpha^{1/9^*} & 1 \end{bmatrix} \otimes \begin{pmatrix} 1 & \beta^{1/9} & \beta^{4/9} & \beta \\ \beta^{1/9^*} & 1 & \beta^{1/9} & \beta^{4/9} \\ \beta^{4/9^*} & \beta^{1/9^*} & 1 & \beta^{1/9} \\ \beta^* & \beta^{4/9^*} & \beta^{1/9^*} & 1 \end{pmatrix}$

For cases with more antennas at either eNB or UE or both, the channel spatial correlation matrix can still be expressed as the Kronecker product of R_{eNB} and R_{UE} according to $R_{spat} = R_{eNB} \otimes R_{UE}$ .The parameters α and β for different correlation types are given in Table 3-11.

Table 3-11: Correlation Values [2]

Low correlation		Medium Correlation		High Correlation	
α	β	α	β	α	β
0	0	0.3	0.9	0.9	0.9

The correlation matrices for high, medium and low correlation are defined in Table 3-12, Table 3-13 and Table 3-14, as below.

Table 3-12: MIMO correlation matrices for high correlation [2]

Antenna config.	Spatial correlation matrix
1x2	$R_{high} = \begin{pmatrix} 1 & 0.9 \\ 0.9 & 1 \end{pmatrix}$
2x2	$R_{high} = \begin{pmatrix} 1 & 0.9 & 0.9 & 0.81 \\ 0.9 & 1 & 0.81 & 0.9 \\ 0.9 & 0.81 & 1 & 0.9 \\ 0.81 & 0.9 & 0.9 & 1 \end{pmatrix}$
4x2	$R_{high} = \begin{bmatrix} 1.0000 & 0.8999 & 0.9883 & 0.8894 & 0.9542 & 0.8587 & 0.8999 & 0.8099 \\ 0.8999 & 1.0000 & 0.8894 & 0.9883 & 0.8587 & 0.9542 & 0.8099 & 0.8999 \\ 0.9883 & 0.8894 & 1.0000 & 0.8999 & 0.9883 & 0.8894 & 0.9542 & 0.8587 \\ 0.8894 & 0.9883 & 0.8999 & 1.0000 & 0.8894 & 0.9883 & 0.8587 & 0.9542 \\ 0.9542 & 0.8587 & 0.9883 & 0.8894 & 1.0000 & 0.8999 & 0.9883 & 0.8894 \\ 0.8587 & 0.9542 & 0.8894 & 0.9883 & 0.8999 & 1.0000 & 0.8894 & 0.9883 \\ 0.8999 & 0.8099 & 0.9542 & 0.8587 & 0.9883 & 0.8894 & 1.0000 & 0.8999 \\ 0.8099 & 0.8999 & 0.8587 & 0.9542 & 0.8894 & 0.9883 & 0.8999 & 1.0000 \end{bmatrix}$
4x4	$R_{high} = \begin{bmatrix} 1.0000 & 0.9882 & 0.9541 & 0.8999 & 0.9882 & 0.9767 & 0.9430 & 0.8894 & 0.9541 & 0.9430 & 0.9105 & 0.8587 & 0.8999 & 0.8894 & 0.8587 & 0.8099 \\ 0.9882 & 1.0000 & 0.9882 & 0.9541 & 0.9767 & 0.9882 & 0.9767 & 0.9430 & 0.9430 & 0.9541 & 0.9430 & 0.9105 & 0.8894 & 0.8999 & 0.8894 & 0.8587 \\ 0.9541 & 0.9882 & 1.0000 & 0.9882 & 0.9430 & 0.9767 & 0.9882 & 0.9767 & 0.9105 & 0.9430 & 0.9541 & 0.9430 & 0.8587 & 0.8894 & 0.8999 & 0.8894 \\ 0.8999 & 0.9541 & 0.9882 & 1.0000 & 0.8894 & 0.9430 & 0.9767 & 0.9882 & 0.8587 & 0.9105 & 0.9430 & 0.9541 & 0.8099 & 0.8587 & 0.8894 & 0.8999 \\ 0.9882 & 0.9767 & 0.9430 & 0.8894 & 1.0000 & 0.9882 & 0.9541 & 0.8999 & 0.9882 & 0.9767 & 0.9430 & 0.8894 & 0.9541 & 0.9430 & 0.9105 & 0.8587 \\ 0.9767 & 0.9882 & 0.9767 & 0.9430 & 0.9882 & 1.0000 & 0.9882 & 0.9541 & 0.9767 & 0.9882 & 0.9767 & 0.9430 & 0.9430 & 0.9541 & 0.9430 & 0.9105 \\ 0.9430 & 0.9767 & 0.9882 & 0.9767 & 0.9541 & 0.9882 & 1.0000 & 0.9882 & 0.9430 & 0.9767 & 0.9882 & 0.9767 & 0.9105 & 0.9430 & 0.9541 & 0.9430 \\ 0.8894 & 0.9430 & 0.9767 & 0.9882 & 0.8999 & 0.9541 & 0.9882 & 1.0000 & 0.8894 & 0.9430 & 0.9767 & 0.9882 & 0.8587 & 0.9105 & 0.9430 & 0.9541 \\ 0.9541 & 0.9430 & 0.9105 & 0.8587 & 0.9882 & 0.9767 & 0.9430 & 0.8894 & 1.0000 & 0.9882 & 0.9541 & 0.8999 & 0.9882 & 0.9767 & 0.9430 & 0.8894 \\ 0.9430 & 0.9541 & 0.9430 & 0.9105 & 0.9767 & 0.9882 & 0.9767 & 0.9430 & 0.9882 & 1.0000 & 0.9882 & 0.9541 & 0.9767 & 0.9882 & 0.9767 & 0.9430 \\ 0.9105 & 0.9430 & 0.9541 & 0.9430 & 0.9430 & 0.9767 & 0.9882 & 0.9767 & 0.9541 & 0.9882 & 1.0000 & 0.9882 & 0.9430 & 0.9767 & 0.9882 & 0.9767 \\ 0.8587 & 0.9105 & 0.9430 & 0.9541 & 0.8894 & 0.9430 & 0.9767 & 0.9882 & 0.8999 & 0.9541 & 0.9882 & 1.0000 & 0.8894 & 0.9430 & 0.9767 & 0.9882 \\ 0.8999 & 0.8894 & 0.8587 & 0.8099 & 0.9541 & 0.9430 & 0.9105 & 0.8587 & 0.9882 & 0.9767 & 0.9430 & 0.8894 & 1.0000 & 0.9882 & 0.9541 & 0.8999 \\ 0.8894 & 0.8999 & 0.8894 & 0.8587 & 0.9430 & 0.9541 & 0.9430 & 0.9105 & 0.9767 & 0.9882 & 0.9767 & 0.9430 & 0.9882 & 1.0000 & 0.9882 & 0.9541 \\ 0.8587 & 0.8894 & 0.8999 & 0.8894 & 0.9105 & 0.9430 & 0.9541 & 0.9430 & 0.9430 & 0.9767 & 0.9882 & 0.9767 & 0.9541 & 0.9882 & 1.0000 & 0.9882 \\ 0.8099 & 0.8587 & 0.8894 & 0.8999 & 0.8587 & 0.9105 & 0.9430 & 0.9541 & 0.8894 & 0.9430 & 0.9767 & 0.9882 & 0.8999 & 0.9541 & 0.9882 & 1.0000 \end{bmatrix}$

Table 3-13: MIMO correlation matrices for medium correlation [2]

Antenna config.	Spatial correlation matrix
1x2	N/A
2x2	$R_{medium} = \begin{pmatrix} 1 & 0.9 & 0.3 & 0.27 \\ 0.9 & 1 & 0.27 & 0.3 \\ 0.3 & 0.27 & 1 & 0.9 \\ 0.27 & 0.3 & 0.9 & 1 \end{pmatrix}$
4x2	$R_{medium} = \begin{pmatrix} 1.0000 & 0.9000 & 0.8748 & 0.7873 & 0.5856 & 0.5271 & 0.3000 & 0.2700 \\ 0.9000 & 1.0000 & 0.7873 & 0.8748 & 0.5271 & 0.5856 & 0.2700 & 0.3000 \\ 0.8748 & 0.7873 & 1.0000 & 0.9000 & 0.8748 & 0.7873 & 0.5856 & 0.5271 \\ 0.7873 & 0.8748 & 0.9000 & 1.0000 & 0.7873 & 0.8748 & 0.5271 & 0.5856 \\ 0.5856 & 0.5271 & 0.8748 & 0.7873 & 1.0000 & 0.9000 & 0.8748 & 0.7873 \\ 0.5271 & 0.5856 & 0.7873 & 0.8748 & 0.9000 & 1.0000 & 0.7873 & 0.8748 \\ 0.3000 & 0.2700 & 0.5856 & 0.5271 & 0.8748 & 0.7873 & 1.0000 & 0.9000 \\ 0.2700 & 0.3000 & 0.5271 & 0.5856 & 0.7873 & 0.8748 & 0.9000 & 1.0000 \end{pmatrix}$
4x4	$R_{medium} = \begin{pmatrix} 1.0000 & 0.9882 & 0.9541 & 0.8999 & 0.8747 & 0.8645 & 0.8347 & 0.7872 & 0.5855 & 0.5787 & 0.5588 & 0.5270 & 0.3000 & 0.2965 & 0.2862 & 0.2700 \\ 0.9882 & 1.0000 & 0.9882 & 0.9541 & 0.8645 & 0.8747 & 0.8645 & 0.8347 & 0.5787 & 0.5855 & 0.5787 & 0.5588 & 0.2965 & 0.3000 & 0.2965 & 0.2862 \\ 0.9541 & 0.9882 & 1.0000 & 0.9882 & 0.8347 & 0.8645 & 0.8747 & 0.8645 & 0.5588 & 0.5787 & 0.5855 & 0.5787 & 0.2862 & 0.2965 & 0.3000 & 0.2965 \\ 0.8999 & 0.9541 & 0.9882 & 1.0000 & 0.7872 & 0.8347 & 0.8645 & 0.8747 & 0.5270 & 0.5588 & 0.5787 & 0.5855 & 0.2700 & 0.2862 & 0.2965 & 0.3000 \\ 0.8747 & 0.8645 & 0.8347 & 0.7872 & 1.0000 & 0.9882 & 0.9541 & 0.8999 & 0.8747 & 0.8645 & 0.8347 & 0.7872 & 0.5855 & 0.5787 & 0.5588 & 0.5270 \\ 0.8645 & 0.8747 & 0.8645 & 0.8347 & 0.9882 & 1.0000 & 0.9882 & 0.9541 & 0.8645 & 0.8747 & 0.8645 & 0.8347 & 0.5787 & 0.5855 & 0.5787 & 0.5588 \\ 0.8347 & 0.8645 & 0.8747 & 0.8645 & 0.9541 & 0.9882 & 1.0000 & 0.9882 & 0.8347 & 0.8645 & 0.8747 & 0.8645 & 0.5588 & 0.5787 & 0.5855 & 0.5787 \\ 0.7872 & 0.8347 & 0.8645 & 0.8747 & 0.8999 & 0.9541 & 0.9882 & 1.0000 & 0.7872 & 0.8347 & 0.8645 & 0.8747 & 0.5270 & 0.5588 & 0.5787 & 0.5855 \\ 0.5855 & 0.5787 & 0.5588 & 0.5270 & 0.8747 & 0.8645 & 0.8347 & 0.7872 & 1.0000 & 0.9882 & 0.9541 & 0.8999 & 0.8747 & 0.8645 & 0.8347 & 0.7872 \\ 0.5787 & 0.5855 & 0.5787 & 0.5588 & 0.8645 & 0.8747 & 0.8645 & 0.8347 & 0.9882 & 1.0000 & 0.9882 & 0.9541 & 0.8645 & 0.8747 & 0.8645 & 0.8347 \\ 0.5588 & 0.5787 & 0.5855 & 0.5787 & 0.8347 & 0.8645 & 0.8747 & 0.8645 & 0.9541 & 0.9882 & 1.0000 & 0.9882 & 0.8347 & 0.8645 & 0.8747 & 0.8645 \\ 0.5270 & 0.5588 & 0.5787 & 0.5855 & 0.7872 & 0.8347 & 0.8645 & 0.8747 & 0.8999 & 0.9541 & 0.9882 & 1.0000 & 0.7872 & 0.8347 & 0.8645 & 0.8747 \\ 0.3000 & 0.2965 & 0.2862 & 0.2700 & 0.5855 & 0.5787 & 0.5588 & 0.5270 & 0.8747 & 0.8645 & 0.8347 & 0.7872 & 1.0000 & 0.9882 & 0.9541 & 0.8999 \\ 0.2965 & 0.3000 & 0.2965 & 0.2862 & 0.5787 & 0.5855 & 0.5787 & 0.5588 & 0.8645 & 0.8747 & 0.8645 & 0.8347 & 0.9882 & 1.0000 & 0.9882 & 0.9541 \\ 0.2862 & 0.2965 & 0.3000 & 0.2965 & 0.5588 & 0.5787 & 0.5855 & 0.5787 & 0.8347 & 0.8645 & 0.8747 & 0.8645 & 0.9541 & 0.9882 & 1.0000 & 0.9882 \\ 0.2700 & 0.2862 & 0.2965 & 0.3000 & 0.5270 & 0.5588 & 0.5787 & 0.5855 & 0.7872 & 0.8347 & 0.8645 & 0.8747 & 0.8999 & 0.9541 & 0.9882 & 1.0000 \end{pmatrix}$

Table 3-14: MIMO correlation matrices for low correlation [2]

Antenna configuration	Spatial correlation matrix
1x2	$R_{low} = \mathbf{I}_2$
2x2	$R_{low} = \mathbf{I}_4$
4x2	$R_{low} = \mathbf{I}_8$
4x4	$R_{low} = \mathbf{I}_{16}$

In Table 3-14, $\mathbf{I}_d$ is the $d \times d$ identity matrix.

For system simulations, large scale fading such pathloss and shadow fading models are necessary, which have been defined by 3GPP. An example for parameters for large scale fading is listed in Table 3-15 for an urban outdoor macrocell scenario. For a detailed description see [4].

Table 3-15: Baseline channel parameters for outdoor macrocell deployments

Parameter	Value
Path Loss (PL) [*R* in meters]	$PL(R) = 128.1 + 37.6 \log_{10} R$
Shadowing standard deviation	8 dB
Shadowing correlation between cells	0.5
Shadowing correlation between sectors	1.0
Autocorrelation distance of shadowing	50 m
Penetration Loss	20 dB if the UE is indoors, otherwise 0 dB

3.1.3.2 Cooperative Channel Models

3.1.3.2.1 Relay-technology deployment scenarios

Relaying is considered for LTE-A as a tool to improve, e.g., the coverage of high data rates, group mobility, temporary network deployment, the cell-edge throughput and/or to provide coverage in new areas. Several scenarios that might benefit from the introduction of relay technology have been discussed in 3GPP [8], as shown in Table 3-16. The decision made was to prioritize for Rel. 10 technologies deployed for coverage extension and enhanced throughput, consisting of fixed outdoor or indoor relays that might be used in one of the first four scenarios in Table 3-16. Issues concerning remaining scenarios are to be addressed in future Releases.

Table 3-16: Application Scenarios for LTE-Advanced Relays [8]

Scenario	Deployment
Rural Area	Achieve ubiquitous coverage whilst reducing deployment cost with the introduction of relays.
Urban Hot Spot	Obtain higher spectrum efficiency while providing coverage enhancement and increased throughput for users. Fixed and nomadic relay nodes are envisaged with this scenario.
Dead Spot	Achieve coverage extension for users in coverage holes. Fixed relay nodes on a planned deployment are envisaged with this scenario.
Indoor Hot Spot	Provide high throughput for indoor hot spots, while maintaining high spectrum efficiency for the system. Throughput requirement can be high and the transmission environment is relatively stationary.
Group Mobility	Mobile relay station intended to facilitate higher throughput and lower handover interruption for local users, who are in a highly mobile public transport (train or bus).
Emergency or Temporary Network Deployment	Coverage scenario for temporary communications network deployment after a disaster or other events that require fast and scalable deployment. Temporary non-emergency deployment may also be required for live events, e.g. fun fair, concerts, public gatherings, sport events, etc.
Wireless backhaul only	RN is deployed for providing backhaul link between eNBs and need not provide access service, i.e., RN provides fixed-point transportation only.

3.1.3.2.2 Multiple-link channel models

The performance assessment of relay-assisted cellular networks depends on the accuracy of the channel models used for the various communication links in the system. Besides the usual eNB-UE link, cooperative relay channels comprise two more communication links, one between eNB and relay node (eNB-RN) and another between relay node and UE (RN-UE). A possible approach to model cooperative relay channels is to use existing point-to-point channel models for each of the three links in the system. Since the LTE-Advanced standardization process aims at developing a candidate IMT-Advanced Radio Interface Technology (RIT) solution, the IMT-Advanced channel model [9] was agreed for the eNB-UE link, such as to have a meaningful set of evaluation results for the ITU-R submission. However, this channel model does not capture the characteristics of relay systems, and cannot be directly applied to eNB-RN and RN-UE links. Indeed, in case of fixed relays, the main difference comes from the height of the RN antenna (much lower than that of eNB but much higher than that of UE), which results in different propagation characteristics. In case of mobile relays, the mobility of the RN will determine specific characteristics of the channel model, especially for the RN-UE link which should be modelled as a (mobile to mobile) channel (however, relay mobility is not addressed in Rel. 10).

3.1.3.2.3 Large scale fading

In order to determine the characteristics of the relay channel for the deployment scenarios described in the previous section, several measurement campaigns and modelling work have been performed within the framework of 3GPP LTE-A. Most effort was concentrated on large-scale fading modelling, which fundamentally determines the expected performance of relay systems. In Rel. 10, new large scale fading models were proposed for relay backhaul link (eNB-RN) and access link (RN-UE) [10], which were adopted for relay simulation methodology in [4]. Large scale fading parameters such as path loss (PL), line of sight (LOS) probability, and shadowing are given in Table 3-17. These parameters correspond to fixed outdoor relay deployment in dense urban (3GPP case 1) environment. Table 3-17 also summarizes the baseline parameters for relay-assisted system simulations.

Table 3-17: Baseline parameters for fixed outdoor relay deployment in dense urban (case 1) [4]

Parameter	Backhaul Link (eNB-RN)	Relay Access Link (RN-UE)
Path Loss (PL) [for 2GHz; distance between nodes R expressed in km]	$PL_{LOS}(R) = 100.7 + 23.5 \log_{10}(R)$ $PL_{NLOS}(R) = 125.2 + 36.3 \log_{10}(R)$	$PL_{LOS}(R) = 103.8 + 20.9 \log_{10}(R)$ $PL_{NLOS}(R) = 145.4 + 37.5 \log_{10}(R)$
	Correction (bonus) for optimized deployment by site planning optimization	
	For LOS : $PL_{LOS}(R)$ (no correction) For NLOS : $PL_{NLOS}(R) - B$, where B = 5dB, for donor macro (from each of its sectors) to RN. [For non-donor cell or non-optimized deployment B = 0dB.]	No correction.
LOS probability [distance between nodes R expressed in km]	$Prob(R) = \min\{0.018/R, 1\} \cdot (1-\exp(-R/0.072)) + \exp(-R/0.072)$	$Prob(R) = 0.5-\min\{0.5, 5\cdot\exp(-0.156/R)\} + \min\{0.5, 5\cdot\exp(-R/0.03)\}$
	Correction for optimized deployment by site planning optimization	
	$1-(1- Prob(R))^N$, where N = 3, for donor macro (from each of its sectors) to RN [For non-donor cell or non-optimized deployment N = 1]	No correction
Lognormal Shadowing	Similar to UMTS 30.03, B 1.41.4 [83]	

Shadowing standard deviation	6 dB	10 dB
Shadowing correlation	Intra-cell correlation: 0 Inter-cell correlation: 0.5	Intra-cell correlation: 0 Inter-cell correlation: 0.5
Penetration Loss	0 dB	20 dB
Carrier Frequency	CF = 2 GHz	
Channel model	If fast fading modelling is disabled in system level simulations for relative evaluations, the impairment of frequency-selective fading channels shall be captured in the physical layer abstraction. For SIMO, the physical layer abstraction is based on TU link curves. For MIMO, the physical layer abstraction is FFS.	
UE speeds of interest	N/A	3 Km/h
Doppler of relay-macro link	Jakes spectrum with 5Hz for NLOS component. LOS component [K=10dB].	N/A
Total BS TX power (Ptotal)	30 dBm @ 10 MHz bandwidth	
UE power class	23dBm (200mW) This corresponds to the sum of PA powers in multiple Tx antenna case	
Inter-cell Interference Modelling	UL: Explicit modelling (all cells occupied by UEs), DL: Explicit modelling else cell power = Ptotal	
Antenna configuration	7dBi antenna gain, directional $A(\theta) = -\min\left[12\left(\frac{\theta}{\theta_{3dB}}\right)^2, A_m\right]$ θ_{3dB} = 70 degrees, A_m = 20 dB. 2 tx, 2 rx antenna ports, or 4 tx, 4 rx antenna ports	5dBi antenna gain, omni directional $A(\theta)$ = 0 dB 2 tx, 2 rx antenna ports
Minimum distance between nodes	≥ 75m	≥ 10m
Min dist. between UE and eNB	≥ 35m	
Minimum distance among RNs	≥ 40m	

3.1.3.2.4 Small scale fading

Due to the limited time, small scale fading modelling has not been addressed in Rel. 10. Existing ITU UMa/UMi (Urban Macro / Urban Micro) models can be used, even if these models may not accurately represent the fast fading characteristics of eNB-RN and RN-UE links. There were however some proposals on fast fading modelling for RN-UE and eNB-RN links [11]. The proposed parameters were based on the data from the similar measurement campaign as for large scale fading modelling above [10]. The methodology is similar to the one used by ITU for fast fading modelling. Probability distribution models have been proposed for the delay spread (DS) and for both angle of departure (AoD) and angle of arrival (AoA). Cross-correlation coefficients have also been derived as follows: angle spread of departure (ASD) to DS, angle spread of arrival (ASA) to DS, ASD to shadow fading (SF), ASA to SF, ASA to ASD, and DS to SF. Some of the proposed small scale fading parameters are summarized in Table 3-18, where the obtained values are also compared with corresponding values for ITU UMa/UMi models (see [11], [12] for more details).

Table 3-18: Delay spread, angle spread parameters for RN-UE and eNB-RN links [12]

	Average Delay Spread (DS) (μs)		**Average spread of AoD (degrees)**		**Average spread of AoA (degrees)**	
	LOS	NLOS	LOS	NLOS	LOS	NLOS
RN-UE	0.089	0.148	18	30	25	36
eNB-RN	0.079	0.174	23	29	35	40
ITU UMa	0.093	0.363	14	26	65	74
ITU UMi	0.065	0.129	16	26	56	69

	Cross-correlation values											
	ASD to DS		**ASA to DS**		**ASA to SF**		**ASD to SF**		**DS to SF**		**ASA to ASD**	
	LOS	NLOS	LOS	NLOS	LOS	NLOS	LOS	NLOS	LOS	NLOS	LOS	NLOS
RN-UE	0.3	0.3	0.5	0	0	0	0	0	-0.8	-0.8	0	0.5
eNB-RN	0	0.6	0.3	0	-0.3	0	0	0	-0.3	-0.3	0	0
ITU UMa	0.4	0.4	0.8	0.6	-0.5	0	-0.5	-0.6	-0.4	-0.4	0	0.4
ITU UMi	0.5	0	0.8	0.4	-0.4	-0.4	-0.5	0	-0.4	-0.7	0.4	0

3.1.3.2.5 Correlation of multiple links

Parameters describing different links of the relay channel may exhibit some degree of correlation, mainly due to common shadowing objects and scatters. At the system-level, the degree of correlation is also dependent on the deployment assumptions such as the heights, densities, and distances of the transmitters and receivers. Only a few investigations dealt with multiple-link correlation, as SF correlation, delay spread correlation, and azimuth correlation. One of the most important system-level correlations is the SF correlation, since it impacts the macro-diversity gain, which is a major benefit of cooperative MIMO systems. The SF correlation factor shown in Table 3-17 is actually inherited from the 3GPP Spatial Channel Model (SCM) [13]. It should be noted that this correlation model is not consistent with the one proposed for the WINNER II channel model [14], which actually constitutes the primary module of the IMT-Advanced channel model. Developing a unified framework to investigate multilink fading correlations has been identified as one of the most important issues to address in cooperative MIMO channel modelling [15], [16].

3.1.4 Key Performance Indicators

In this section the key performance indicators (KPIs) at Physical Layer level for the LTE networks are analysed. The KPIs have been defined considering the minimum requirements set by ITU for IMT-Advanced systems [3] and considering also the results obtained in 3GPP during the study item on the CoMP (Coordinated Multipoint Transmission) technique [4].

In particular the minimum requirements set by ITU in terms of average cell spectrum efficiency and cell edge user spectrum efficiency are summarized in Table 3-19 for the different test environments [3]. The microcellular environment is the reference for the small cells deployment scenarios studied within the project.

Table 3-19: ITU minimum requirements in terms of spectrum efficiency [3]

Cell Average Spectral Efficiency		
Test environment	**Downlink (bit/s/Hz/cell)**	**Uplink (bit/s/Hz/cell)**
Indoor	3.0	2.25
Microcellular	2.6	1.8
Base coverage urban	2.2	1.4
High speed	1.1	0.7
Cell Edge user Spectral Efficiency		
Test environment	**Downlink (bit/s/Hz/user)**	**Uplink (bit/s/Hz/user)**
Indoor	0.1	0.07
Microcellular	0.075	0.05
Base coverage urban	0.06	0.03
High speed	0.04	0.015

In Table 3-20, Table 3-21, and Table 3-22, a summary of the performance results obtained in 3GPP has been presented for a microcellular scenario (UMi) during the study item on CoMP. The CoMP technique is suitable for the application in dense networks, where several RAPs (Radio Access Points) are able to transmit or receive towards/from a given UE. Besides, the availability of a suitable level of centralized processing facilitates the coordination at PHY, MAC, and/or RRC level among different transmission points distributed over the coverage area.

Table 3-20: Performance of DL CS/CB-CoMP 4 x 2 (antenna configuration C) (UMi, FDD) [4]

Results from Various Companies in [4]	Cell spectral efficiency (bit/sec/Hz/cell)	Cell-edge user spectral efficiency (bit/sec/Hz/user)
Source 3	2.84	0.092
Source 11	3.11	0.086
Source 12	2.99	0.114
Source 13	3.21	0.084
Source 18	3.15	0.083
Rel-8 SU-MIMO (4 x 2, *L*=3)[1]	2.14	0.068
ITU requirement	2.60	0.075

In particular, Table 3-20 shows the spectrum efficiency results of a 4-by-2 MIMO downlink configuration with Coordinated Scheduling/Beamforming schemes and eNB antenna configuration C (co-polarized vertical antennas with 0.5λ spacing) [4]. The duplexing configuration for the results presented hereafter is FDD.

Similarly Table 3-21 shows the spectrum efficiency results of 4-by-2 MIMO downlink configuration with Joint Processing (JP-CoMP) schemes and eNB antenna configuration C.

[1] *L* is the number of OFDM symbols in each subframe dedicated to the transmission of control information

Table 3-21: Performance of DL JP-CoMP 4 x 2 (antenna configuration C) (UMi, FDD) [4]

Results from Various Companies in [4]	Cell spectral efficiency (bit/sec/Hz/cell)	Cell-edge user spectral efficiency (bit/sec/Hz/user)
Source 1	3.45	0.108
Source 2	3.06	0.097
Rel-8 SU-MIMO (4 x 2, L=3)	2.14	0.068
ITU requirement	2.60	0.075

Concerning the uplink Table 3-22 shows the spectrum efficiency results of 2-by-4 MIMO uplink CoMP schemes with eNB antenna configuration A (co-polarized vertical antennas with 4λ spacing) [4].

Table 3-22: Performance of UL CoMP 2 x 4 (antenna configuration A) (UMi, FDD) [4]

Results from Various Companies in [4]	Cell spectral efficiency (bit/sec/Hz/cell)	Cell-edge user spectral efficiency (bit/sec/Hz/user)
Source 1	2.45	0.102
Source 18	2.18	0.102
Rel-8 SIMO (1 x 4)	1.93	0.074
ITU-R requirement	1.80	0.050

The Table 3-23 reported below provides a list of KPIs at PHY level according to the SotA applicable to the LTE Release 8 networks currently under deployment and LTE-A networks respectively. The average cell spectrum efficiency and the cell edge user spectrum efficiency are suitable metrics for measuring the performance of a wireless dense network including the effect the radio access technology and of the backhauling network. According to the definition provided in the Table these two metrics are derived from the Cumulative Distribution Function (CDF) of the cell and user throughput respectively, as shown in Figure 3-11.

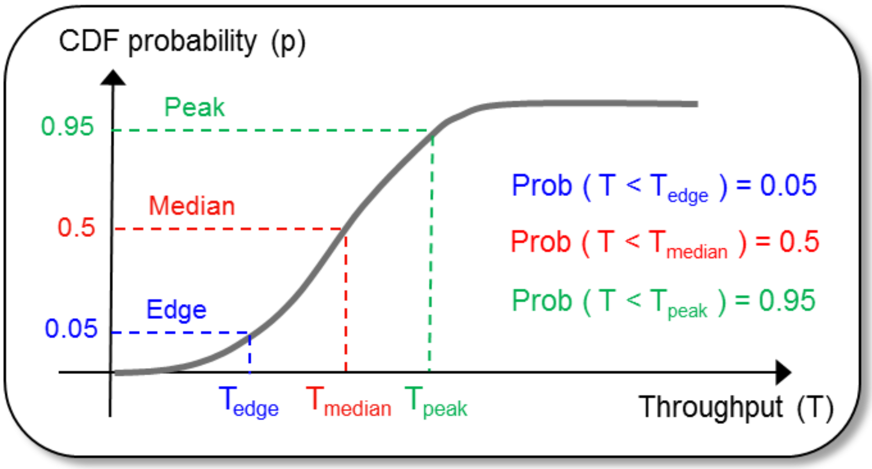

Figure 3-11: Cumulative distribution function of the cell/user throughput

Concerning the user mobility, not indicated in the Table, it seems reasonable to consider the classes of stationary, pedestrian and Vehicular (with speed up to 30 km/h) as suitable for the dense network scenario. Finally, the latency objective has been set below the requirement defined for LTE in [5] but the actual value is expected to depend on the specific technology used for backhauling, as reported in the 3GPP Study Item on Small Cell enhancements [6].

Table 3-23: Key performance indicator at PHY level

Name	Definition	LTE Release 8	LTE Advanced
Max. user rate	Maximum data rate that can be delivered to one user	150 Mbps (DL, MIMO 2x2, 20 MHz, UE category 4) 50 Mbps (UL, SIMO 1x2, 20 MHz, UE category 4)	1 Gbps (DL) 500 Mbit/s (UL)
U-plane Latency	Defined as the one-way transit time between an SDU packet being available at the IP layer in the user terminal/base station and the availability of this packet at IP layer in the base station/user terminal assuming an unloaded network.	5 – 10 ms	< 5 ms (t.b.d.) Note: depends also on used backhauling technology
Average cell spectrum efficiency	Defined as the aggregate throughput of all users (the number of correctly received bits over a certain period of time) normalized by the overall cell bandwidth and divided by the number of cells. Measured in bit/s/Hz/cell.	>1.6 – 2.1 bit/s/Hz/cell (DL with MIMO 2x2 Spatial Multiplexing and IRC receivers) >0.66-1 bit/s/Hz/cell (UL with SIMO 1x2 and IRC receivers)	> 2.6 bit/s/Hz/cell (DL Microcellular coverage) t.b.d. > 1.8 bit/s/Hz/cell (UL Microcellular coverage) t.b.d
Cell Edge user spectrum efficiency	Defined as the 5% point of CDF of the user throughput normalized with the overall cell bandwidth. Measured in bit/s/Hz/user	>0.04 – 0.06 bit/s/Hz/user (DL with 10 users per cell) >0.02 – 0.03 bit/s/Hz/user (UL with 10 users per cell)	> 0.075 bit/s/Hz/cell (DL Microcellular coverage) t.b.d. > 0.05 bit/s/Hz/cell (UL Microcellular coverage) t.b.d

3.2 PHY State of the art for Radio Access

3.2.1 Distributed and iterative multiuser detection

The problem of distributed Multi-User Detection (MUD) has been receiving interest from the academic world for quite a long time now; e.g., in [17] a thorough survey can be found, which will be summarised in the following. In 1994, first information-theoretic investigations have been made [18], the principle of belief propagation was proposed for distributed decoding [19], [20], [21], [22]. This approach requires the iterative exchange of likelihood values or extrinsic information among all involved BSs. Of course, this causes a very large traffic on the backhaul, which is particularly disadvantageous in typical star network topologies.

Alternatively, so-called “Distributed antenna systems” (DAS) were proposed in [23], where the signals received at these distributed antennas are forwarded to a processing centre, where they are jointly detected and decoded. This technique can provide a SINR (signal-to-interference-and-noise ratio) gain, but also has the drawback of large resulting backhaul traffic, as was pointed out in [24].While it is acknowledged that a distributed MUD can provide an optimum detection, amends to practical backhaul constraints have to be made. In [17], the authors investigate the different options for information exchange among cooperating BSs: the least backhaul-intensive option is to exchange hard bits, e.g., preliminarily estimated payload data. The better option from information theoretic point of view is to exchange data with corresponding reliability information. This can be accomplished by either exchanging Log Likelihood Ratios (LLRs) or soft-bits. According to [17], a trade-off between detection quality and amount of information exchanged on the backhaul can be achieved by varying the quantisation of the exchanged information.

In [25] the authors propose a distributed ICI cancellation technique that uses the turbo principle. This approach uses the exchange of soft-bits among base stations. Here, also quantisation is suggested for the reduction of resulting backhaul traffic.

3.2.2 Inter-Cell Interference Coordination (ICIC) and Coordinated Multi-Point Transmission (CoMP)

It is well-known that the capacity of single-user MIMO systems increases linearly with the minimum of transmit and receive antennas at high signal-to-noise ratio (SNR) [54], [55]. Using joint pre-coding (downlink) or decoding (uplink), the sum capacity of multi-user MIMO can be increased linearly even when each mobile user has single antenna [56], [57]. However, in a realistic cellular system presence of inherent ICI reduces SNR of the cell-edge users. Therefore, the dramatic increase in sum capacity through MIMO cannot be realized in a cellular system. In order to combat ICI and achieve capacity gains, various techniques have been proposed in the literature [58]. Among these techniques, BS cooperation or CoMP in 3GPP has gained much popularity in recent few years.

In CoMP, BSs in adjacent cells cooperate with each other before sending data to their users [59]. This transforms the interference-limited channels to noise-limited and hence the capacity of cell-edge users can be enhanced. Depending upon the level of cooperation between the BSs, CoMP techniques have been categorized as follows by 3GPP [4].

1. **Joint Processing:**
   In this transmission scheme, each BS (involved in cooperation) or RAP for example has data and channel-state-information (CSI) of each user. Therefore, each user receives information signals from all the RAPs coherently. In this way, ICI is converted into useful signal provided that perfect synchronization exists between the cooperative RAPs. Moreover, this transmission scheme comes with large backhaul (J1 or J2 links in iJOIN terminology) overheads and stringent synchronization requirements.

2. **Coordinated Beamforming (CB):**
   In this case, each RAP has data of its own local cell users but also has CSI of all the users present in the cooperative cells. Hence, each RAP performs its own individual precoding. Since only CSI needs to be shared among the cooperative RAPs, backhaul overheads are relatively less when compared to joint-processing at the expense of reduction in sum access capacity.

3. **Coordinated Scheduling:**
   This scheme is also known as “inter-cell scheduling” [59]. ICI is avoided because in one time/frequency resource, only one RAP is scheduled to transmit. The attractive feature of this scheme is that the message exchange among the RAPs is comparable to that of handoff which is already employed in cellular systems. The most promising advantage of coordinated scheduling is to achieve expanded multiuser diversity, however, due to transmission duty cycle reduction; this scheme is not optimal [59]

Dirty paper coding (DPC) with joint processing (also known as multi-cell DPC) is first proposed in [60]. Although DPC is capacity-achieving, it is not suitable for implementation in practice due to its high complexity. Motivated by this fact, several multi-cell linear precoding techniques are discussed in [61] with both total and per BS power constraints. Even though in CoMP transmission, per BS constraint is a more realistic assumption, it has been shown that sum capacity degrades due to this per BS power constraint. However, besides ICI mitigation potential, CoMP provides some other additional benefits; for example power gain, channel rank/conditioning advantage, and macro diversity protection for shadowing channels [61]. The maximum achievable common rate in a coordinated network with zero-forcing (ZF) and DPC is analysed in [62] and [63]. Similarly, it is also shown in [64] that joint processing improves the sum access capacity considerably.

The backhaul overhead and feedback requirements in FDD increase proportional to the number of cooperative RAPs, number of antennas per base-station and number of users. Therefore, for a large network, different strategies have been proposed in literature to reduce burden of these overheads. Among these strategies, one approach which has been extensively studied is clustering. In clustering, the numbers of RAPs are limited to cooperate only within the cluster and inter-cluster signals are considered as interference. Multi-cell Block Diagonalization (BD) is used in [65] for joint processing within the same cluster. Moreover, in order to satisfy the per BS power constraint, three different power allocation algorithms are proposed in [65].

In [66], adaptive switching between single-cell beamforming (also known as maximum ratio transmission) and ZF is proposed to enhance the sum rate. It is shown that less feedback is required for this adaptive scheme when compared to the static ZF. Moreover, the impact of channel quantization (for CSI feedback) is also quantified in [66].

Besides clustering, coordinated beamforming (as mentioned above) is also used to reduce backhaul overhead when compared to joint processing [67]. In [67], an efficient algorithm is proposed to design optimal global beamformers for all the RAPs without need to exchange data of other cell users. Beamformers are designed to minimize either weighted sum power or maximum per BS power subject to SINR constraints at the users.

In practice, the backhaul capacity is limited and therefore joint processing is not always superior to coordinated beamforming. Sum capacity is analysed for different cooperative schemes under backhaul constraints in [68], [69], and [70]. A new rate splitting scheme is proposed in [69] in which each RAP splits its message into two parts: common part and private part. Only a common part is shared between the RAPs and thus reduces the backhaul overhead. It is shown through simulations in [70] that coordinated beamforming outperforms joint processing when the backhaul capacity is low and /or the edge SNR is high. Motivated by this fact, semi-dynamic mode selection between joint processing and coordinated beamforming is proposed in [71] with different random user and orthogonal user scheduling schemes.

Inter-cell scheduling is studied in [59] and it is shown that opportunistic scheduling in multi-cell systems achieve an expanded multi-user diversity due to independent log-normal shadowing in each cell. Therefore, inter-cell scheduling outperforms static frequency reuse (which is used in conventional cellular systems) technique while having the same complexity. Besides this performance improvement, through inter-cell scheduling universal frequency can be adopted and hence frequency planning is not required [59].

The main benefits of CoMP transmission are

- **Interference Handling:** Joint processing has the potential to turn the interference into useful signal. On the other hand, coordinated beamforming may enable the clustering entities to cooperate so as to avoid the ICI.
- **Better user experience:** The joint reception from multiple RAPs or sites using CoMP techniques enables the overall received power at the handset to be increased which directly translates into large throughput and better user experience.
- **Improved Network Utilization:** By providing connections to several RAPs at once, using CoMP, data can be passed through least loaded RAPs for better resource utilization.
- **Better Channel Rank:** By joint processing, the channel rank is generally being improved as compared to single-cell scenario, and this results in higher capacity [61].
- **Macro diversity Protection:** Joint processing also provides macro diversity protection for shadowing channels because shadowing is generally uncorrelated among the cooperative RAPs.

3.2.3 Joint network-channel coding

By exploiting the broadcast nature and the inherent spatial diversity of wireless communications, Sendonaris et al. introduced the concept of cooperative diversity [29], [30] over wireless relay channels and their multi-terminal extensions. Subsequently, many authors proposed cooperation protocols for the relay channel, which can be classified into two major categories, namely the amplify-and-forward (AF) and the decode-and-forward (DF) [31]. In AF protocols, the relay simply amplifies the received signal and forwards it to the destination. The DF protocol allows the relay to decode the received signal, re-encode it, and forward it to the destination. The forwarded message can either be identical to, or part of the initial transmission (repetition coding), or it can be obtained by using a dedicated coding scheme at the relay (distributed coding). In the first case the destination combines received signals both from source and relay, which results in an improved SNR on the received transmission. Besides, the same code is used for encoding at the source and decoding at the destination. In the second case, the destination gains knowledge of extra information, but it needs a dedicated decoding scheme, able to jointly decode received signals from both source and relay. Distributed turbo and low density parity check (LDPC) codes for the relay channel have been proposed in [32] – [39].

For both AF and DF protocols, the amount of data transmitted by the relay (e.g. expressed in number of transmitted bits) is usually equal to the amount of data initially transmitted by the source. This may be particularly problematic in case of multiple access relay channels (MARC), i.e. when the same relay is simultaneously used by several users to communicate with the destination, especially if the relay-to-destination link has limited capacity. In order to overcome this limitation, network coding (NC) can be advantageously used at the relay. Instead of separately relaying data packets for each of the users accessing the channel, the NC technique [40] allows combining them together for transmission. Although it was first proposed in the context of error-free networks as a technique to achieve the maximum possible information flow, NC proved also to be particularly useful in the context of wireless networks, allowing significant improvements in network's throughput [41].

An example of MARC with 2 sources, 1 relay and 1 destination is depicted in Figure 3-12. It illustrates the case when 2 UEs use a common "relay" (RAP1 node) to communicate with a final destination (RAP2/eNB), and only concern uplink transmissions. UEs' transmissions are encoded by two channel codes C_1 and C_2, while a network code C is used at the relay. The destination decodes the received signals using knowledge of C_1, C_2 and C. Consequently, a joint-design of network (C) and channel (C_1, C_2) codes is desired in order to fully exploit these two coding techniques. Several joint network channel coding (JNCC) schemes have been proposed in the literature [42] – [51]. While these works investigate the design of effective JNCC schemes using either Turbo or LDPC channel coding, they do not elaborate on a structure to guarantee full diversity (at maximum rate) of the proposed joint code design. The maximum achievable coding rate that allows to achieve full diversity when NC is not used at the relay is R_c = 1/2. The use of NC yields an increase of the maximum full diversity rate from R_c = 1/2 to R_c = 2/3. A rate 2/3 full-diversity JNCC design for the MARC, based on root-LDPC codes, has been recently proposed in [52], [53].

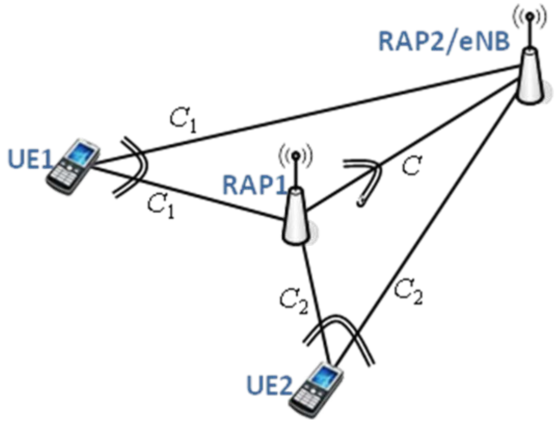

Figure 3-12: Example of a multiple access relay channel (MARC)

3.2.4 Frequency-domain RoF

The RoF solution is a widely known approach for current radio base station layouts, but it has also so-called "horizontal" applications, namely applications where it is used for implementing particular radio access architectures. These solutions are feasible provided that a good availability of fibre in terms of deployed fibre networks usually in urban environments is assumed and they can represent a possible building element for any "cloud" oriented architectural solutions.

Many studies and initiatives have been put forward recently on this topic. In particular there have been some standardization works in the past, among which Common Public Radio Interface (CPRI) [72] and Open Base Station Architecture Initiative (OBSAI) [73] were the most considered (see IR5.1 for details about them). These works are carried on by an ETSI group, called ORI ("Open Radio Interface") that disclosed a phase 1 specification in 2012 and is now working on a phase 2, with advanced topics in the agenda [82].

In one of the studies, among the others, performed in ORI phase 2, they treat the issue regarding the compression techniques of data to be transmitted over the fibre links (the data rate in the ORI format is usually much higher than in the backhauling). These techniques will be briefly discussed in section 3.3.1, but frequency domain RoF (FD-RoF) is definitely to be classified as one of them, representing de facto a reduction in the data rate requested transmission. Details about frequency domain RoF will be given in section 4.7.

3.3 PHY State of the art for Backhauling

Traditionally, various technologies have been in use for backhauling operation. Backhauling has been used as the operation of information exchange between the core network and network nodes at the end of the network. Some of the technologies which have served as backhaul are free space optical communication, point-to-point microwave links and digital subscriber lines etc. Fibre optic based backhauling has been used for a long time, offering very large data rates. mmWave backhauling is getting more and more attention these days because of its ability to serve as flexible backhaul. 3GPP has standardized in-band and out-of-band relaying as a sort of backhaul. In the following, we detail these interesting backhaul candidate technologies.

3.3.1 Fibre-based backhauling

As stated in section 3.2.4, the transmission of data over fibre is generally known as radio over fibre (RoF), if the so-called “front-hauling” is considered, and in such a context the data rate to be transmitted is greater than in the “traditional” backhauling, i.e. on top of the radio access part element and towards the core network.

Regarding traditional fibre based backhauling, it is commonly based on Gigabit Ethernet solutions, or with dedicated fibres in some deployments. In such cases, compression techniques or methods are seldom used, due to the intrinsic lower data rate with respect to the fronthauling. A global overview of the possible backhauling solutions for LTE as an example is given in [75] and [76].

Instead, for the fronthauling some solutions to compress data are more and more necessary to cope with the growing capacity requested by new radio access technologies (RATs) and also by multi RAT solutions. Examples of the data rates that are requested by fronthauling for different RATs are reported in [75] and [76].

In these white papers a dedicated algorithm to compress data is used and some results are shown. Other options are based on approaches similar to the one that will be discussed in section 4.7 about FD-RoF and they are not based on compression of data, usually degrading the quality of the transmission, but on alternatives splitting interfaces in the transceiver chain. The FD-RoF uses the interface before the IFFT in the transceiver, for LTE case, but one could decide to interpose the fibre even before in the transceiver (considering the downlink), achieving different performances but in general reducing the data rate to be transmitted over the fibre with respect to the case of traditional CPRI or ORI standard.

3.3.2 Wireless and mmWave backhauling

For wireless backhauling a number of frequency bands have been considered so far. Apart from in-band backhaul, the available solutions can be separated into traditional microwave (6-42 GHz), sub-6-GHz microwave, unlicensed (60 GHz) and licensed (70-80 GHz) millimetre wave systems. Furthermore, free space optics (FSO) can also be considered as wireless backhaul [77].

Generally speaking, wireless backhaul has the advantage that it is easier, faster and cheaper to deploy than wired backhaul. On the other hand, it usually offers lower data rate and lower availability. However, the different wireless systems have widely different characteristics themselves [78].

- Free space optics offer high data rates of multiple Gbps due to the very high available bandwidth and usually do not have to be licensed, lowering cost and deployment time. However, they suffer heavily from snowfall and fog, limiting either range or availability. Due to their very narrow beamwidth, they also have to be carefully aligned and are susceptible to thermal expansion, building sway, and vibration. When they are facing east to west, they can also suffer from sunlight effects [78].
- Traditional microwave systems can only offer low data rates below 1 Gbps and use licensed spectrum, increasing costs and deployment time. The 5 GHz band is also used by many users as it is specified as a WiFi band. This increases interference, which further limits data rates and decreases availability. The 5 GHz system is also the one most vulnerable to interception, because all other systems use highly directive beams that would require an interceptor be suspiciously deployed in the connection’s LOS.
- The 60 GHz band offers up to 9 GHz of unlicensed spectrum, allowing for multi- Gbps data rates and fast deployment. However, 60 GHz faces a uniquely high attenuation through oxygen absorption and rain, limiting its range to below 2 km. In contrast, the oxygen absorption has the advantage that

interference between 60 GHz links is very low, especially if combined with narrow antenna beams. This also increases the security against eavesdropping. However, the small beamwidth limits multipath effects, making spatial diversity multiplexing techniques more difficult and also requires line of sight.

- The 70- 80 GHz band combines the advantages of high bandwidth, long range and high availability. The spectrum is licensed, yet the licensing process is (at least in the US) easy and affordable. It also shares the advantages and disadvantages of narrow antenna beams with 60 GHz systems. However, since it is the highest frequency system considered, hardware design is the most challenging.

To increase reliability, different wireless backhauls can be combined, e.g., a 60 GHz system as main link and a 5 GHz link as backup in case of heavy rain. As in any communication system, effective data rates can be lowered in favour of a more robust coding, to ensure connectivity in suboptimal situations.

An overview of the different technologies is provided in Table 3-24.

Table 3-24: Overview over wireless backhaul technologies

Parameter	**<6GHz**	**6-42 GHz**	**60 GHz**	**70/80 GHz**	**FSO**
Typical data rate	400 Mbps	400 Mbps	1 Gbps (commercial) 10 Gbps (demonstrator)	1 Gbps (commercial) 10 Gbps (demonstrator)	1 – 10 Gbps
Typical range	<5 km (interference limited)	5 km	0.1 – 1 km	3 km	1 km
Licensing	Licensed/ unlicensed (5.8 GHz)	licensed	unlicensed	"lightly" licensed	unlicensed
Other	Multipath for spatial diversity High interference Easy to intercept		Very low interference Oxygen attenuation NLOS might not be possible	NLOS might not be possible	High degree of alignment required Only LOS possible high attenuation by snow, fog

The link budget of microwave (28 GHz) and millimetre-wave (72 GHz) backhaul links for several cases is given in Table 3-25.

Table 3-25: Link Budget for 28 and 72 GHz frequencies [79]

Parameters	Case 1	Case 2	Case 3	Case 4
TX Power (dBm)	35.00	35.00	25.00	25.0
TX antenna gain (dBi)	30.00	30.00	30.00	30.00
Carrier frequency (GHz)	28.00	72.00	28.00	72.00
Distance (km)	1.00	1.00	0.50	0.50
Propagation Loss (dB)	121.34	129.55	115.32	123.53
Other losses	20.00	20.00	20.00	20.00
RX antenna gain (dBi)	15.00	15.00	15.00	15.00
Received power (dBm)	-61.34	-69.55	-65.32	-73.53
Bandwidth (GHz)	1.00	1.00	1.00	1.00
Thermal PSD(dBm)	-174.00	-174.00	-174.00	-174.00
Noise Figure (dBm)	10.00	10.00	10.00	10.00
Thermal Noise (dBm)	-74.00	-74.00	-74.00	-74.00
SNR (dB)	12.66	4.45	8.68	0.47
Implementation Loss (dB)	5.00	5.00	5.00	5.00
Data rate (Gb/s)	2.77	0.91	1.74	0.4

3.3.3 In-band backhauling

One important characteristic of an LTE relay node (RN) is the carrier frequency it operates on. Two operation modes can be distinguished:

- **Inband:** An LTE relay node is said to be inband if the eNB-RN link shares the same carrier frequency with RN-UE links.
- **Outband:** In this case the eNB-RN link does not operate in the same carrier frequency as RN-UE links.

Depending on the relaying strategy, a relay may either be part of the donor cell or control a cell of its own. Accordingly, the following types of LTE relays can be distinguished [4]:

- **Type 1:** Such RNs control their cells with their own identity including the transmission of their own synchronisation channels and reference symbols. To ensure backwards compatibility, Type 1 RNs appear as if they are a Rel. 8 eNB to Rel. 8 UEs. The basic Type 1 LTE relay provides half duplex with inband transmissions.
- **Type 1.a:** These RNs have the same properties as the basic Type 1 RNs, except that they operate outband in full duplex mode.
- **Type 1.b:** These RNs have the same properties as the basic Type 1 RNs, except that they operate inband (with adequate antenna isolation) in full duplex mode.
- **Type 2:** These RNs do not have their own cell identity and look just like the main cell. Any UE in range is not able to distinguish a RN from the main eNB within the cell. Control information can be transmitted from the eNB and user data from the RN. The RN operates inband in full duplex mode.

The main properties of the different relaying types are summarized in Table 3-26.

Table 3-26: Relay Types in 3GPP LTE Rel.10

LTE Relay Type	Cell ID	Frequency spectrum	Duplex mode
Type 1	Yes	Inband	Half duplex
Type 1.a	Yes	Outband	Full duplex
Type 1.b	Yes	Inband	Full duplex
Type 2	No	Outband	Full duplex

RN-eNB link for inband relay Type 1: In order to allow inband relaying, some resources in the time-frequency space are set aside for the backhaul link (Un) and cannot be used for the access link (Uu). The following resource partitioning scheme is mandatory in 3GPP LTE Rel. 10.

General principle for resource partitioning at the relay:

- eNB → RN and RN → UE links are time division multiplexed in a single carrier frequency (only one is active at any time)
- RN → eNB and UE → RN links are time division multiplexed in a single carrier frequency (only one is active at any time)

Multiplexing of backhaul links in FDD:

- eNB → RN transmissions are done in the DL frequency band
- RN → eNB transmissions are done in the UL frequency band

Multiplexing of backhaul links in TDD:

- eNB → RN transmissions are done in the DL subframes of the eNB and RN
- RN → eNB transmissions are done in the UL subframes of the eNB and RN

RN-eNB link for inband relay Type 1b: If the outgoing and incoming signals at the RN are adequately isolated in the spatial domain, e.g., by appropriate arrangement of the respective antennas for the Un and Uu links, the eNB→ RN and RN→ UE (RN→ eNB and UE→ RN) links can be activated simultaneously without the need for the time division multiplexing. The operation of Type 1b relay nodes may not be supported in all deployment scenarios.

RN-eNB link for outband relay: If RN-eNB and RN-UE links are isolated enough in frequency (possibly with help of additional means such as antenna separation), then there is no interference issue in activating both links simultaneously. Therefore, it becomes possible for relay-eNB link to reuse the channels designed for UE-eNB link.

4 PHY Candidate Technologies

In this section we define the PHY technologies for the radio access network and the backhaul network that are promising candidates to meet the challenges of dense deployment of small cells. These CTs enable a holistic design of radio access network and backhaul network. Table 4-1 summarizes the CTs per partner of WP2.

Table 4-1: List of iJOIN PHY Candidate Technologies (CTs)

CT	Partner	Topic
2.1	UoB	In-Network-Processing
2.2	SCBB	Multipoint Turbo Detection
2.3	CEA	Joint Network-Channel Coding
2.4	UNIS	Sum-Rate and Energy-Efficiency Metrics of DL COMP with backhaul constraints
2.5	IMC	Cloud Based Joint-Processing and Partially Centralized Inter-Cell Interference Coordination
2.6	TI	Data Compression over RoF
2.7	TUD	60 GHz backhauling

The following table lists, which CT will be applied to which of the iJOIN CS defined in IR5.1. As a partner may change his interest with respect to the uses cases to be investigated, this given assignment is preliminary and up to further changes. Here, “x” means that the CS will be considered, whereas “o” denotes that the CS may be considered.

Table 4-2: Mapping of PHY CTs to iJOIN Common Scenarios (CS)

Scenario	2.1 UoB	2.2 SCBB	2.3 CEA	2.4 UNIS	2.4 IMC	2.5 TI	2.6 TUD
CS 1 Stadium		o	o	x		x	x
CS 2 Square	x	o			x	o	x
CS 3 Wide-area continuous coverage			x	o		x	x
CS 4 Indoor (Airport / Shopping Mall)	x	x		x	x	o	

In the subsequent sections the different candidate technologies are described and the preliminary set of assumptions and requirements per CT are listed. In the given tables, “x” indicates mandatory assumptions (requirements), “*” represents optional choices for the implementation if several options are possible, whereas “o” denotes optional assumptions, i.e., not-mandatory features that may lead to improvements.

Before going into the details of each CT, it is important to provide brief description about the iJOIN architecture and define the entities used in this architecture. The preliminary draft of the iJOIN architecture is shown in Figure 4-1.

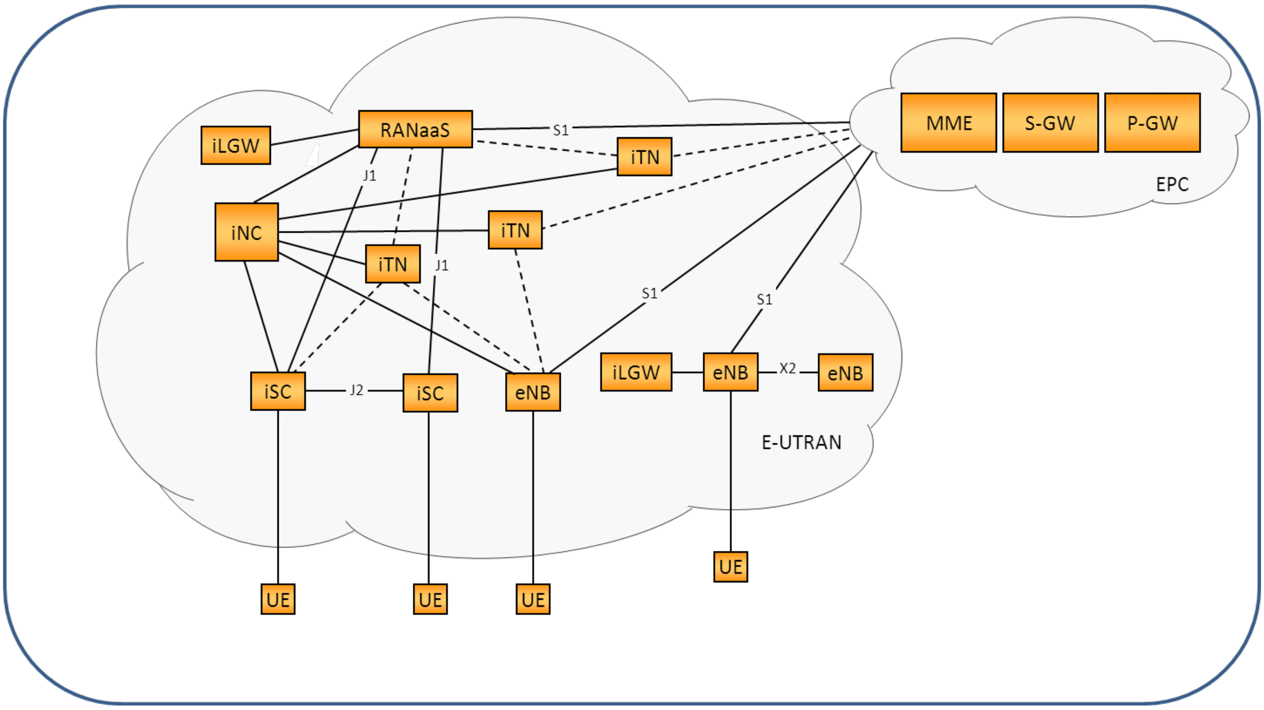

Figure 4-1: Preliminary draft of the iJOIN Architecture

4.1 iJOIN Entities

4.1.1 RAN as a Service (RANaaS)

Cloud computing platform allowing centralisation processing and/or functional split of the lower OSI layer(s) (L1/L2/L3) usually process in a base station.

4.1.2 iJOIN Small Cell (iSC)

Low power flexible radio access point implementing fully or partially the lower OSI layer(s) (RF/L1/2/3) of a base station (upper layers being handled by the RANaaS platform for partial implementation). It shares all other properties of a small cell. There may be different implementations of an iSC, e.g.:

- L0-iSC (or RF-iSC) only handles the RF transmission (equivalent to an analogue or digital RRH);
- L1-iSC handles all functionalities below Layer 1 and part or all functionalities of Layer 1;
- L2-iSC handles all functionalities below Layer 2 and part or all functionalities of Layer 2;
- L3-iSC handles all functionalities below Layer 3 and part or all functionalities of Layer 3 (if all Layer 3 functionalities are handled, then the L3-iSC is equivalent to a classical SC).

4.1.3 Virtual eNB

It includes all small cell functionalities. A virtual eNB can (logically and physically) coincide with an eNB or can be implemented as a split between RANaaS and iSC.

4.1.4 iJOIN Network Controller (iNC)

A functionality (or logical entity) for the control of joint RAN/backhaul (BH) and/or RANaaS/iSC split. In order to minimize the impacts for the operator in terms of deployment cost and complexity, the iNC should preferably be physically co-located with the RANaaS entity.

4.1.5 iJOIN Local Gateway (iLGW)

An entity implementing a subset of the logical functions of a P-GW, it is logically connected with the eNB, but that can be physically located somewhere in the RAN.

4.1.6 iJOIN Transport Node (iTN)

This is an entity between iSC and RANaaS, or eventually between RAN and core network (possibly connected as mesh network).

4.1.7 J1/J2 interfaces

J1 is the logical interface between RANaas and iSCs. Furthermore, J2 is the logical interface through which iSCs communicate and exchange information with each other directly.

4.2 CT 2.1: In-network processing

4.2.1 Scenario description

The objective of the investigated In-Network-Processing techniques is to increase the user throughput, and therefore, also the area throughput. Correspondingly, the UE transmit power is intended to be reduced if the user throughput is kept unchanged.

In order to facilitate this, a UE is assumed to be in the range of several iSCs, with overlapping cells. The iSCs in general will be L1-iSCs, but could also be higher layer iSCs. These iSCs cooperate in the detection process by exchanging information with each other. This information can be raw symbols, LLRs, soft bits or decided "hard" bits. The type of exchanged information is subject of the investigations, as well as its actual specificity, its amount, its actual exploitation in the algorithm etc.

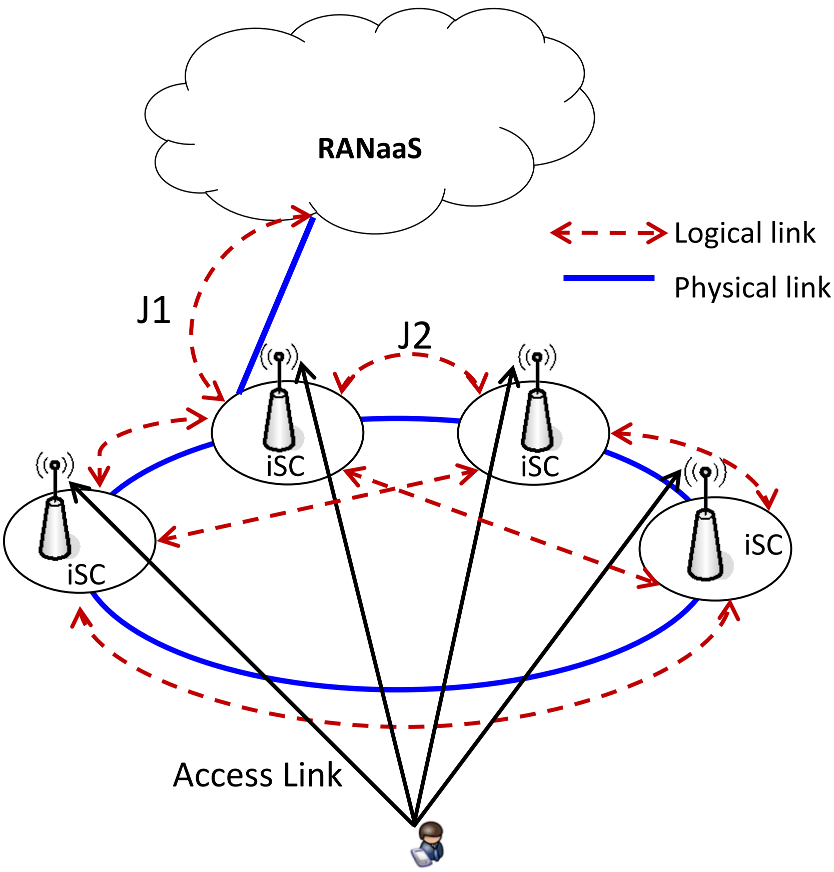

Figure 4-2: A UE is served by several iSCs, cooperating through In-Network-Processing

4.2.2 Assumptions

We assume that iSCs may have arbitrary physical connections to the core network or with each other.

A J1 interface is assumed to be available between the RANaaS platform and iSCs, since it is required for centralised processing ("in-cloud", one extreme of the functional split): information on receive signals have to be carried on this logical interface (either raw samples, LLRs, or hard decided data). The underlying nature of the physical link does not need to be specified, as long as its latency/bandwidth properties are known.

Furthermore, we assume the presence of a J2 interface between at least some (but not necessarily all) iSCs for decentralised processing: Also on this logical link information on receive signals (see above) has to be carried. Its properties are also known.

Figure 4-2 illustrates the envisioned scenario and shows the different logical interfaces between iSCs and RANaaS. The preliminary set of assumptions for CT2.1 is summarized in Table 4-3.

Table 4-3: Assumptions of CT2.1: In-network processing

Assumption	Description	
A.1	Large number of iSCs in local area	x
A.2	Availability of macro BS in same frequency band (co-channel deployment)	o
A.4	J1 interface between <u>all</u> iSCs and RANaaS with known parameters	o
A.5	J1 interface between <u>some</u> iSCs and RANaaS with known parameters	x
A.6	J2 interface for interconnections of all iSCs	o
A.7	J2 interface for interconnections of some iSCs (direct neighbours, selection)	x
A.8	Wired inter-node links between iSCs (fibre)	*
A.9	Wireless inter-node links between iSCs (60GHz)	*
A.10	Wired connection of iSCs to RANaaS (fibre)	*
A.11	Wireless connection of iSCs to RANaaS (60GHz)	*
A.12	Availability of a logical controller (iNC) for the joint RAN/BH optimization	x
A.2.4	Local RxCSI at iSCs	x
A.2.6	LTE Modulation & Coding Schemes	x
A.2.10	Uplink Transmission	x
A.2.13	Multiple Tx/Rx antennas at iSC	o

4.2.3 Technology requirements

J1 and J2 are required to expose a very low latency, since several iterations of the In-Network-Processing Algorithms need to be carried out per received UE frame. Furthermore, all iSCs are required to be perfectly synchronised, since the distributed algorithm needs to run synchronously on all involved iSCs.

The preliminary set of requirements for CT2.1 is summarized in Table 4-4.

Table 4-4: Requirements of CT2.1: In-network processing

Technical requirement	Description	
R.2.1	Limited capacity for J1 links (high, medium, low)	x
R.2.2	Limited capacity for J2 links (high, medium, low)	x
R.2.3	Low latency for J1 links (zero, very small, small)	x
R.2.4	Low latency for J2 links (zero, very small, small)	x
R.2.5	Perfect synchronization among iSCs (perfect, limited)	x
R.2.6	Message exchange between iSCs for distributed processing	x
R.2.9	Large coherence time of channels, i.e. slowly varying channels	x
R.2.16	Local RxCSI at iSCs (perfect, imperfect)	x

4.2.4 iJOIN objectives addressed

The main iJOIN objectives addressed are:

- Increase of area throughput: The use of a distributed receive processing results in an improved joint detection of several users and therefore a reduction in effective interference. This allows for an increase of area throughput.
- Reduction of power consumption: With reception through several iSCs in parallel, the required transmit power of the UE to achieve a certain performance can be reduced, therefore increasing battery life and consequently, reducing the power consumption.

4.3 CT 2.2: Multipoint turbo detection

4.3.1 Scenario description

This scenario will investigate the benefit of relying on the turbo detection principle to increase the (aggregated) user throughput in the uplink direction. In a dense small cell deployment, one user can see other small cells in addition to its serving one, especially if he is at the edge of the cell. Under such condition, if co-channel deployment is used due to limited spectrum, classical approach tends to create orthogonality in the frequency domain for OFDMA-based systems through soft or fractional frequency reuse patterns among neighbouring small cells. By nature, this orthogonality reduces the spectrum available for transmission, meaning fewer throughputs in theory.

By scheduling the (edge) users on the same resources and exploiting the created interference as a source of information through the turbo detection principle in each concerned small cell, the (aggregated) throughput should be improved, as “more” spectrum and diversity are made available.

Since turbo detection is an extensive computational process, the RANaaS platform could be used if the link toward this platform supports the data transfer required (raw I/Q, compressed/uncompressed CSI, LLRs ...). If this link does not support such data flow to be transmitted, turbo processing could be done locally at each iSC with some information exchange.

The investigation will evaluate the performance provided by the multipoint turbo detection method and try to identify the amount and the type of information to be exchanged to allow a scalable application of this algorithm based on the iSC/RANaaS platform link capability. In order to do so, the deployment shown in Figure 4-3 will be investigated to perform link-level simulations. Other deployment may also be investigated (such as two users and one small cell only or one user and two small cells).

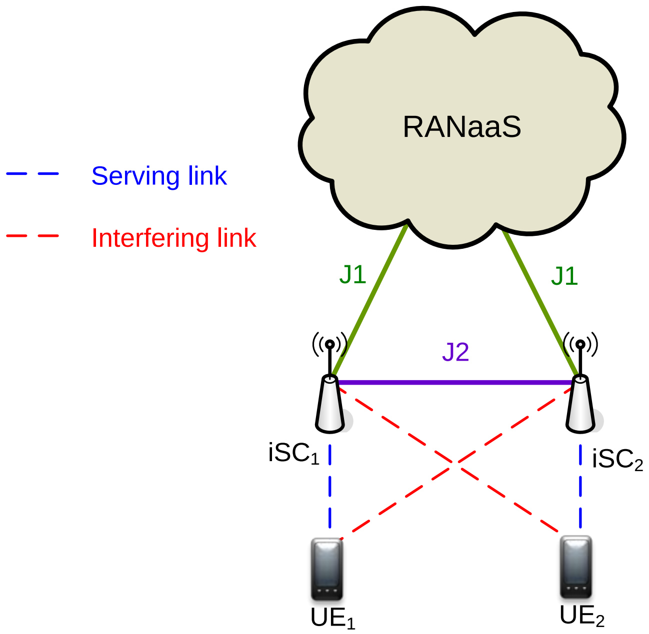

Figure 4-3: Multipoint turbo detection investigation context

4.3.2 Assumptions

- Inter-connected small cells
- Based on the J1 capacity/latency, information will be exchanged between small cell and RANaaS platform for the latter to perform the turbo detection
- Based on the J2 capacity/latency (if J1 is not high capacity enough); information (TBD) between small cells may be exchanged

The preliminary set of assumptions for CT2.2 is summarized in Table 4-5.

Table 4-5: Assumptions of CT2.2: Multipoint turbo detection

Assumption	Description	
A.1	Large number of iSCs in local area	x
A.4	J1 interface between all iSCs and RANaaS with known parameters	x
A.6	J2 interface for interconnections of all iSCs	*
A.8	Wired inter-node links between iSCs (fibre)	*
A.9	Wireless inter-node links between iSCs (60GHz)	*
A.10	Wired connection of iSCs to RANaaS (fibre)	*
A.11	Wireless connection of iSCs to RANaaS (60GHz)	*
A.12	Availability of a logical controller (iNC) for the joint RAN/BH optimization	o
A.2.3	Global RxCSI at RANaaS	x
A.2.4	Local RxCSI at iSCs	x
A.2.6	LTE Modulation & Coding Schemes	x
A.2.10	Uplink Transmission	x
A.2.13	Multiple Tx/Rx antennas at iSC	o

4.3.3 Technology requirements

- Time/Frequency synchronized small cell
- High processing power at the RANaaS platform if J1 has sufficient capacity/latency requirements

The preliminary set of requirements for CT2.2 is summarized in Table 4-6.

Table 4-6: Requirements of CT2.2: Multipoint turbo detection

Technical requirement	Description	
R.2.1	Limited capacity for J1 links (high, medium, low)	x
R.2.2	Limited capacity for J2 links (high, medium, low)	*
R.2.3	Low latency for J1 links (zero, very small, small)	x
R.2.4	Low latency for J2 links (zero, very small, small)	*
R.2.5	Perfect synchronization among iSCs (perfect, limited)	x
R.2.6	Message exchange between iSCs for distributed processing	*
R.2.7	Message exchange between iSCs and RANaaS (CPU) for partly distributed processing	x
R.2.8	Message forwarding of iSCs to RANaaS (CPU) for centralized processing	x
R.2.9	Large coherence time of channels, i.e. slowly varying channels	x
R.2.11	Preferably fibre-based J1 and J2 interfaces	x

R.2.15	Global RxCSI at RANaaS (CPU) (perfect, limited, imperfect)	x
R.2.16	Local RxCSI at iSCs (perfect, imperfect)	x

4.3.4 iJOIN objectives addressed

- Area Throughput (other objectives TBC after definition) should be increased by a better detection and spectrum utilisation.

4.4 CT 2.3: Joint network-channel coding

4.4.1 Scenario description

The proposed scenario concerns uplink transmissions and is depicted in Figure 4-4. As shown in this figure, two or more UEs use a common intermediate iSC1 to communicate with a final destination (iSC2 or macro-cell eNB). UEs' transmissions are encoded by two channel codes C_1 and C_2, while a network code C is used at the relay. The destination decodes the received signals using knowledge of C_1, C_2 and C.

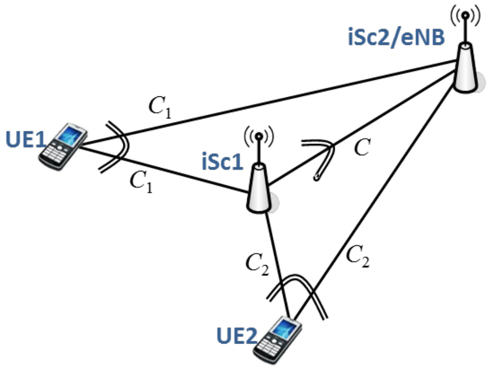

Figure 4-4: Proposed scenario for joint network channel coding.

The use of the joint network channel coding (JNCC) is aimed at increasing the users' throughput in the uplink direction, and it is particularly suitable when the intermediate iSC1 has limited resources to supply the users it serves with the services they demand. If a more distant iSC2 has available backhaul resources (e.g. iSC2 serves a smaller number of users than iSC1), it can take over responsibility of the backhaul access for users UE1 and UE2. The drawback is that the users are penalized by the increasing distance to iSC2 node, which generally results in a degraded capacity of the wireless UEs-iSC2 links. However, iSc1 can help increasing the users' throughput, by providing iSC2 with additional data pertaining to the user transmissions. Since the additional data is actually provided by the network code used at iSC, the whole coding scheme can be optimized such as to minimize the amount of data to be transmitted on the iSC1 to iSC2 link, subject to a target throughput for users UE1 and UE2.

The goal of the investigation is to propose a joint-design of network (C) and channel (C_1, C_2) codes, such that to fully exploit the spatial diversity of the multiple access relay channel, while reducing the traffic-load on the relay-to-destination (iSC1-iSC2) link. The joint-design is illustrated in Figure 4-5 where $X_i = C_i(U_i)$, and $X = C(U_1, U_2)$ are the code words generated by the cannel codes (C_1, C_2) and the network code C, respectively.

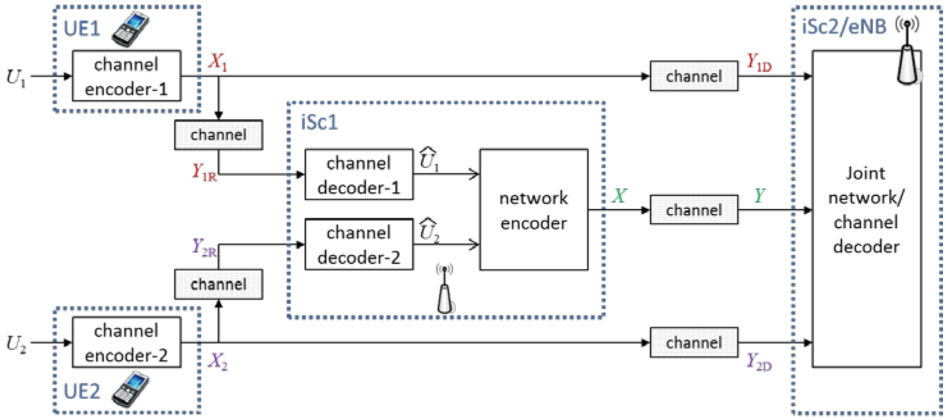

Figure 4-5: Joint Network Channel coding for the MARC

4.4.2 Assumptions

- iSCs are connected with each other and at least some are connected to the RANaaS.
- J1 interface between iSCs and RANaaS required for centralised processing
- J2 interface between iSCs required for decentralised processing

The preliminary set of assumptions for CT2.3 is summarized in Table 4-7.

Table 4-7: Assumptions of CT2.3: Joint network channel coding

Assumption	Description	
A.2	Availability of macro BS in same frequency band (co-channel deployment)	*
A.4	J1 interface between all iSCs and RANaaS with known parameters	*
A.5	J1 interface between some iSCs and RANaaS with known parameters	x
A.7	J2 interface for interconnections of some iSCs (direct neighbours, selection)	x
A.9	Wireless inter-node links between iSCs (60GHz)	x
A.11	Wireless connection of iSCs to RANaaS (60GHz)	x
A.2.2	Local TxCSI at iSCs	x
A.2.4	Local RxCSI at iSCs	x
A.2.6	LTE Modulation & Coding Schemes	*
A.2.9	Adaptive Coding and Modulation	x
A.2.10	Uplink Transmission	x

4.4.3 Technology requirements

- Wireless (and possibly resource-limited) backhaul link
- Synchronization between iSCs/eNBs

The preliminary set of requirements for CT2.3 is summarized in Table 4-8.

Table 4-8: Requirements of CT2.3: Joint network channel coding

Technical requirement	Description	
R.2.1	Limited capacity for J1 links (high, medium, low)	x
R.2.2	Limited capacity for J2 links (high, medium, low)	x
R.2.5	Perfect synchronization among iSCs (perfect, limited)	x

R.2.6	Message exchange between iSCs for distributed processing	x
R.2.7	Message exchange between iSCs and RANaaS (CPU) for partly distributed processing	o
R.2.8	Message forwarding of iSCs to RANaaS (CPU) for centralized processing	o
R.2.9	Large coherence time of channels, i.e. slowly varying channels	o

4.4.4 iJOIN objectives addressed

- Increase of the area throughput.

4.5 CT 2.4: Sum-Rate and Energy-Efficiency metrics of DL COMP with backhaul constraints

4.5.1 Scenario description

In this scenario, geographically dispersed iSCs cooperate with each other to form a "Virtual MIMO" (e.g., joint processing) and hence convert cell-edge interference into useful signal. Moreover, iSCs can exchange users' CSI and perform coordinated beamforming/scheduling and hence avoid interference. This coordination or cooperation between the iSCs takes place through dedicated backhaul links either in a centralized way with the help of a central unit (RANaaS terminology in iJOIN) as shown in Figure 4-6 or in a decentralized fashion, shown in Figure 4-7. In both these figures, solid green lines represent signals intended for respective users, whereas red dot-dashed lines are the interfering signals from neighbouring cells. Backhaul links (both J1 and J2) are represented by the dashed green lines.

In this work, the trade-off between the backhaul capacity and sum-rate will be quantified considering the fact that some system resources are utilized during backhauling. Initially, wired backhaul will be assumed which will later be extended to wireless backhaul. The analysis will cover both cases of infinite / finite backhaul capacity. Moreover, it will be studied that how much gain in sum-rate (or energy efficiency) can be achieved by investing system resources (or in terms of cost) for backhauling. Since CSI is required at the iSCs, the impact of limited or imperfect CSI on the performance gain will be analysed. Furthermore, in order to maximize the sum-rate for a given backhaul capacity, adaptive selection of joint processing and coordinated beamforming will be proposed.

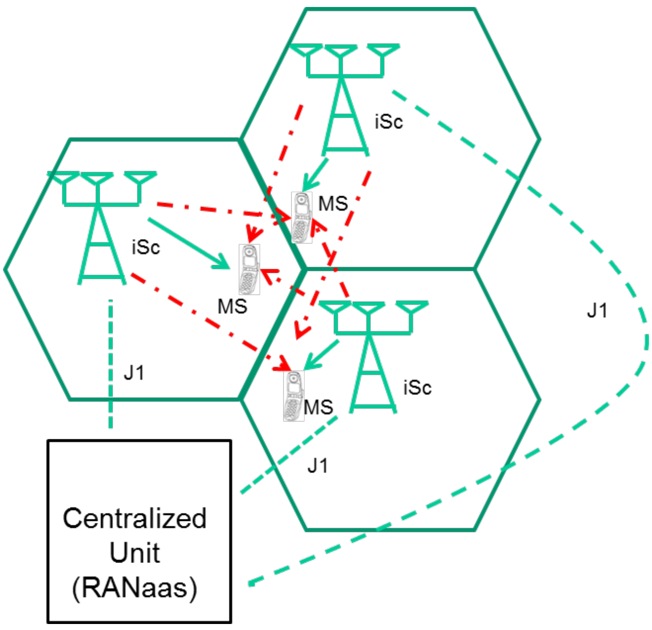

Figure 4-6: A three cell network with limited backhaul capacities of J1 links (centralized architecture).

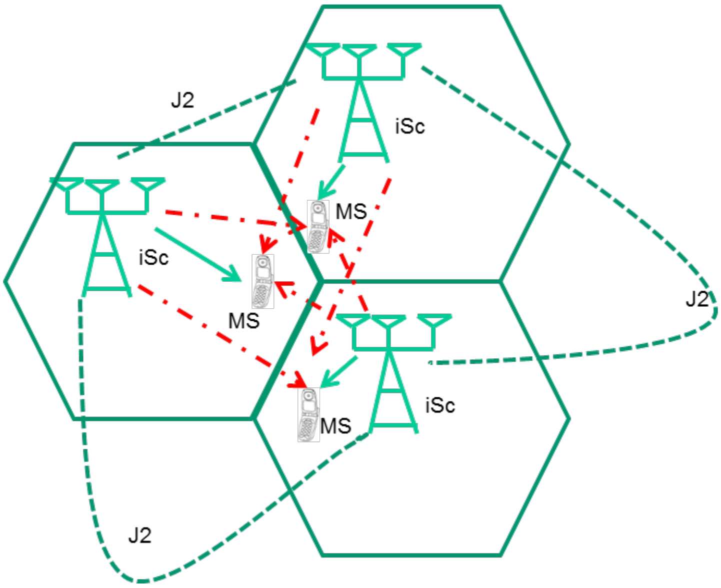

Figure 4-7: Each iSC is connected with each other through J2 interfaces (de-centralized architecture).

4.5.2 Assumptions

Coordination and information exchange between iSCs is carried out on J2 interfaces for decentralized architecture. In case of centralized architecture, coordination between RANaas and iSCs takes place using J1 interfaces.

The preliminary set of assumptions for CT2.4 is summarized in Table 4-9.

Table 4-9: Assumptions of CT2.4: Sum-rate and Energy efficiency metrics of DL-COMP

Assumption	Description	
A.1	Large number of iSCs in local area	x
A.4	J1 interface between all iSCs and RANaaS with known parameters	x
A.6	J2 interface for interconnections of all iSCs	o
A.7	J2 interface for interconnections of some iSCs (direct neighbours, selection)	o
A.8	Wired inter-node links between iSCs (fibre)	o
A.9	Wireless inter-node links between iSCs (60GHz)	o
A.10	Wired connection of iSCs to RANaaS (fibre)	o
A.11	Wireless connection of iSCs to RANaaS (60GHz)	*
A.12	Availability of a logical controller (iNC) for the joint RAN/BH optimization	o
A.2.1	Global TxCSI at RANaaS	x
A.2.2	Local TxCSI at iSCs	x
A.2.7	Gaussian Input Signals	x
A.2.8	Perfect Channel Codes (infinite length)	x
A.2.11	Downlink Transmission	x
A.2.12	FDD / TDD	x
A.2.13	Multiple Tx/Rx antennas at iSC	x

4.5.3 Technology requirements

Large (but limited) capacity is assumed for the J1/J2 interfaces. Furthermore, it is assumed that J1/J2 links have very low latency and thus will not be considered for the analytical framework of access capacity.

The preliminary set of requirements for CT2.4 is summarized in Table 4-10

Table 4-10: Requirements of CT2.4: Sum-rate and Energy efficiency metrics of DL-COMP

Technical requirement	Description	
R.2.1	Limited capacity for J1 links (high, medium, low)	x
R.2.2	Limited capacity for J2 links (high, medium, low)	x
R.2.3	Low latency for J1 links (zero, very small, small)	x
R.2.4	Low latency for J2 links (zero, very small, small)	x
R.2.5	Perfect synchronization among iSCs (perfect, limited)	x
R.2.6	Message exchange between iSCs for distributed processing	x
R.2.7	Message exchange between iSCs and RANaaS (CPU) for partly distributed processing	o
R2.8	Message forwarding of iSCs to RANaaS (CPU) for centralized processing	o
R.2.9	Large coherence time of channels, i.e. slowly varying channels	x
R.2.12	LOS between iSC and RANaaS	o
R.2.13	Global TxCSI at RANaaS (CPU) (perfect, limited, imperfect)	x
R.2.14	Local TxCSI at iSCs (perfect, limited, imperfect)	x
R.2.17	~2 GHz of BW on 60 GHz link	o

4.5.4 iJOIN objectives addressed

- Improvements in spectral efficiency/ energy efficiency using DL CoMP.

4.6 CT 2.5: Cloud Based Joint-Processing and Partially Centralized Inter-Cell Interference Coordination

4.6.1 Scenario description

In a network deployment where the access side has very dense deployment of small cells and RANaaS cloud functionality is available, many novel and flexible PHY layer techniques can be envisioned to enhance the system performance and user experience. This candidate technology CT2.5 targets a hot spot scenario which could for example be a big square in down-town (CS2) or an indoor dense one which could be a busy shopping mall or inside an airport (CS4). The general setting would be the availability of dense iSCs covering the area and the presence of many users which need to be served. This kind of scenario would require the aggressive frequency reuse at iSCs which would eventually result in strong interference conditions if not dealt properly.

This candidate technology CT2.4 assumes the presence of J2 links between neighbouring iSCs and the J1 links connecting iSCs to RANaaS nodes. Depending upon a large set of system variables, users'/applications' data requirements, users' locations, channel conditions experienced by individual users, capacity and latency of J1 and J2 links, various levels of cooperation strategies can be adopted at iSCs, a subset of whom might require processing at RANaaS nodes.

In the downlink direction, in the presence of large bandwidth and low latency (relative mainly to channel variation mechanism) J1 links, very sophisticated Network MIMO version of CoMP approaches can be implemented in the cloud. This approach reduces the part of the network where it is adopted to a single transmitter having distributed antennas with individual per-antenna power constraints. Then different coordination rules need to be defined and enforced between multiple of these clusters to tackle the inter-cluster interference. In the investigation, a network realized by heterogeneous backhaul links with different capacity and latency parameters would be investigated. In such a setting, network MIMO kind of approaches are hard to implement on a large cluster due to physical constraints and the focus would be to investigate cooperation strategies with clustering enabled and with acceptable information exchanges. This interference coordination can be enabled in small clusters through RANaaS. One other possibility is to exploit the presence of J2 links where iSCs can exchange partial channel state information to better combat the interference situations.

As outlined above, this particular network architecture gives rise to a number of joint transmission and interference handling possibilities. The discussion above clearly points out the fact that there exists a non-trivial optimization problem to choose the optimal PHY strategy for enhanced system performance taking into account the constraints of heterogeneous backhaul. Note that the Figure 4-8 is indicative and does not show all possible links/situations.

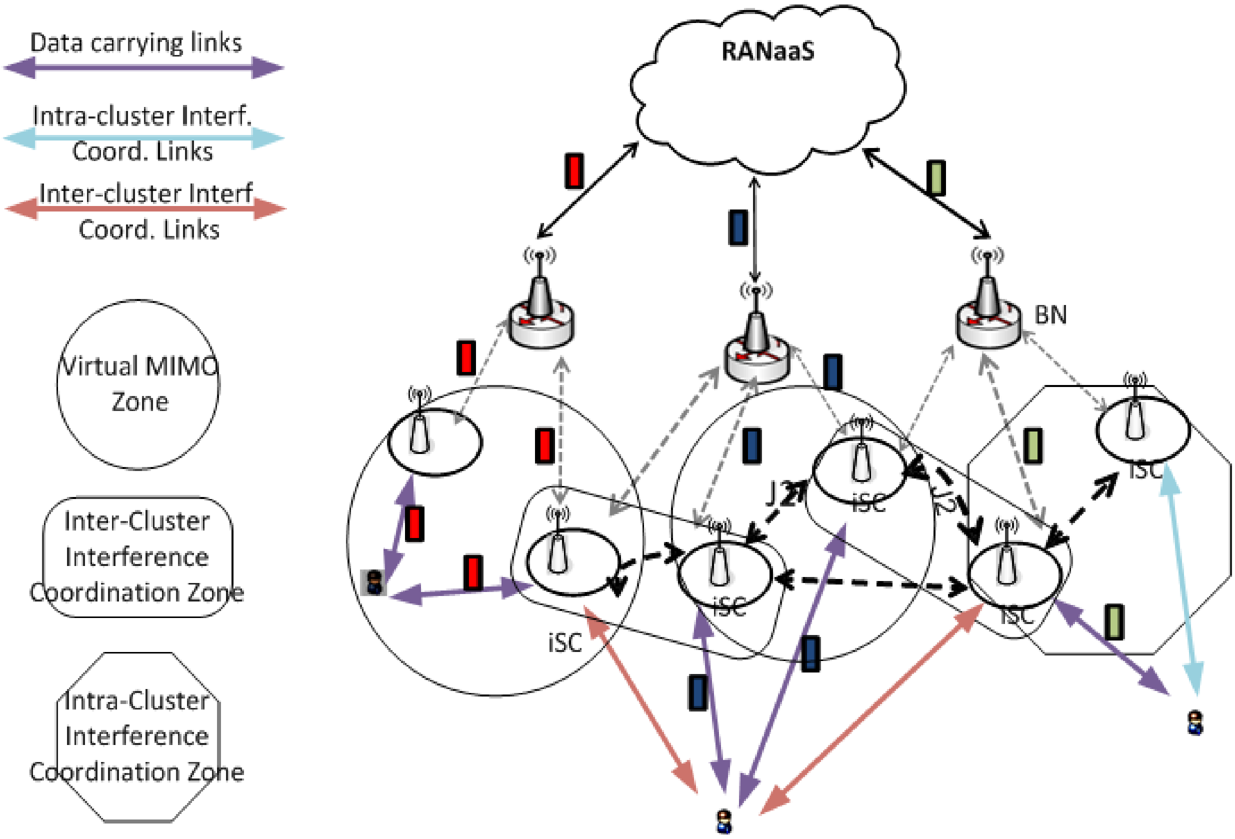

Figure 4-8: An exemplary scenario showing joint transmission and interference coordination.

4.6.2 Assumptions

The preliminary set of assumptions for CT2.5 is summarized in Table 4-11.

Table 4-11: Assumptions of CT2.5: Cloud based Joint processing and partially centralised ICIC

Assumption	Description	
A.1	Large number of iSCs in local area	x
A.2	Availability of macro BS in same frequency band (co-channel deployment)	o
A.4	J1 interface between all iSCs and RANaaS with known parameters	x
A.6	J2 interface for interconnections of all iSCs	o
A.7	J2 interface for interconnections of some iSCs (direct neighbours, selection)	x
A.8	Wired inter-node links between iSCs (fibre)	*
A.9	Wireless inter-node links between iSCs (60GHz)	*
A.10	Wired connection of iSCs to RANaaS (fibre)	*
A.12	Availability of a logical controller (iNC) for the joint RAN/BH optimization	x

A.2.1	Global TxCSI at RANaaS	o
A.2.2	Local TxCSI at iSCs	x
A.2.3	Global RxCSI at RANaaS	o
A.2.4	Local RxCSI at iSCs	x
A.2.5	Global RxCSI at iSCs	o
A.2.7	Gaussian Input Signals	x
A.2.8	Perfect Channel Codes (infinite length)	x
A.2.13	Multiple Tx/Rx antennas at iSC	o

4.6.3 Technology requirements

The preliminary set of requirements for CT2.5 is summarized in Table 4-12.

Table 4-12: Requirements of CT2.5: Cloud based Joint processing and partially centralised ICIC

Technical requirement	Description	
R.2.1	Limited capacity for J1 links (high, medium, low)	x
R.2.2	Limited capacity for J2 links (high, medium, low)	x
R.2.3	Low latency for J1 links (zero, very small, small)	x
R.2.4	Low latency for J2 links (zero, very small, small)	x
R.2.5	Perfect synchronization among iSCs (perfect, limited)	x
R.2.7	Message exchange between iSCs and RANaaS (CPU) for partly distributed processing	x
R.2.8	Message forwarding of iSCs to RANaaS (CPU) for centralized processing	x

4.6.4 iJOIN objectives addressed

- Increase of area throughput.
- Energy efficiency optimization.

4.7 CT2.6: Data compression over RoF

4.7.1 Scenario description

The deployments of dense networks based on a large number of small cells bring two main problems: the interference among the radio access points that limits the spectrum efficiency and the availability of high capacity backhauling connections.

The problem of the interference can be mitigated through the adoption of coordinated transmission techniques like CoMP where several iSCs coordinate their transmission/reception towards/from a given UE. The capacity of the backhauling can be instead increased by leveraging on the structure of the OFDMA and SC-FDMA signals that are transmitted on the downlink and uplink of the LTE/LTE-A system, respectively.

In the following we consider a network architecture based on Radio over Fibre (RoF), which is composed by a central unit RANaaS where the baseband processing is concentrated. The RANaaS is connected by means of fibre links to a large number of radio access points distributed over the coverage area. The access points are in the form of iSCs that are small and easy to install on the existing urban infrastructure of the operator like cabinets, phone boots, lampposts, etc.

In a conventional RoF architecture, the central unit performs the signal processing operations of traditional base station equipment including the higher layer protocols (RRC/RLC/MAC) and the physical layer (L1) signal processing operations up to the generation of the composite digital baseband signal, as shown in

Figure 4-9. The composite digital baseband signal is converted from electrical to optical (E/O) and transmitted over the fibre.

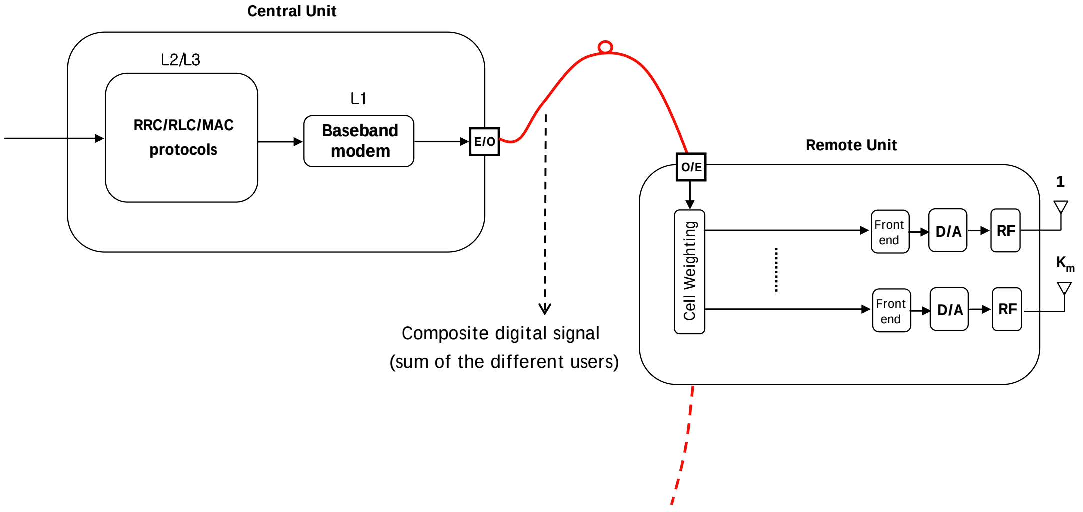

Figure 4-9: Conventional RoF architecture

The iSC receives the composite baseband signal that is first converted from optical to electrical (O/E). The signal is first subject to a weighting operation that operates on cell basis (i.e. for all the users camped or served by the iSC). The weighting operation is optional (i.e. in conventional iSC implementations may not be present) and its purpose is to shape the radiation diagram of the iSC antenna in order to optimize the coverage. For example some antenna parameters, like vertical tilt or 3dB azimuth beamwidth, can be adapted in a semi-static way under the control of the RANaaS.

After the cell weighting operation the signal is then filtered by a front-end, converted from digital to analogue form (D/A), up-converted from baseband to radio frequency (RF), amplified by a power amplifier and radiated by the antennas. The previous signal processing steps refer to the downlink. In the uplink the inverse operations are performed both in the iSC and the RANaaS and the signal transmitted over the optical fibre is still a composite signal formed by the sum of the different user signals. In case of a radio access technology like LTE or LTE-A, the time domain signal at the output of the IFFT module at the transmitter is sent over the optical fibre link. In that case the composite baseband signal, which is made by the sum of the various user signals, can be transmitted over the optical fibre link by using standard transmission formats defined by international consortia such as CPRI (Common Public Radio Interface) [72] or OBSAI (Open Base Station Architecture Initiative) [73].

An estimate of the backhauling capacity required for the transmission of one LTE carrier over the fibre link is easily obtained considering the characteristics of the OFDM signal. The signal at the IFFT output is sampled with a frequency of 30.72 MHz in case of a 20 MHz carrier [74]. The signal is typically oversampled by a factor two, so that the sampling frequency of the signal transmitted on the fibre is 61.44 Mbit/s. Besides, two signals must be transmitted when considering a MIMO 2xN antenna configuration (i.e. with 2 antennas at the iSCs). Finally, assuming that the quantization of the In-phase (I) and Quadrature (Q) components of the OFDM signal is done using 10 bits, it is possible to estimate throughput T_f on the fibre

$$T_f = \underbrace{2}_{\substack{\text{number of}\\ \text{RU antennas}}} \cdot \underbrace{61.44}_{\substack{\text{sampling}\\ \text{frequency}}} \cdot \underbrace{2}_{\substack{\text{I/Q}\\ \text{components}}} \cdot \underbrace{10}_{\substack{\text{signal}\\ \text{quantization}}} = 2.46\,\text{Gbit/s}$$

The value calculated above shows that the backhauling may become a potential bottleneck when considering a scenario with a large number of small cells, or a MIMO configuration with a large number of antennas or also a multi-RAT scenario. The obtained value must be compared with the throughput that can be provided by the different technologies used for backhauling. The Table 4-13 derived from [6] provides a categorization of the different backhauling technologies (i.e., typical backhaul widely used in the market). A further categorization of the backhauling technologies can be also found in [75]. The analysis of the throughput that can be carried by the current backhauling technologies shows that only a limited number of LTE carriers can be transmitted over a fibre link or alternatively only a limited number of iSCs can be connected over a unique fibre link. It then follows that the data compression techniques for increasing the transmission efficiency over the backhauling are of paramount importance for the dense network scenarios.

Table 4-13: Categorization of non-ideal backhaul [6]

Backhaul categories	Latency (one way)	Throughput
Fibre Access 1	10 – 30 ms	10 M – 10 Gbps
Fibre Access 2	5 – 10 ms	100 – 1000 Mbps
DSL Access	15 – 60 ms	10 – 100 Mbps
Cable	25 – 35 ms	10 – 100 Mbps
Wireless Backhaul	5 – 35 ms	10Mbps – 100 Mbps typical, maybe up to Gbps range

Besides, the conventional RoF architecture shown in Figure 4-9 is highly non-efficient when it is necessary to perform signal processing operation on a per-user basis, like for example adaptive beamforming or coordinated transmission between multiple iSCs. In this context the weight factors are different for each user and they have to be continuously updated in order to track the movement of the user within the cell and to track the channel variations. The signal processing algorithms operating on user basis consist in separately multiplying each user signal at the different antenna branches for complex weight factors before the signals are radiated in downlink, or before the signals received from the different antennas are combined in uplink. The application of these algorithms in the small cells, especially in case of dense scenarios limited by the interference, can provide significant gains in terms of throughput and quality of service perceived by the users.

The application of these algorithms in a conventional RoF architecture requires performing all the signal processing operations in the RANaaS prior to the IFFT operation, where the signals of different users are still separately available. As already mentioned, this architecture lacks of flexibility because it is necessary to transmit one composite signal for each antenna element of each iSC. It follows that, as the number of iSCs connected via one link increases, the available transmission capacity on the fibre becomes rapidly a bottleneck.

To cope with the problems listed above it is possible to define a new RoF architecture, denoted as Frequency Domain RoF (FD-RoF) that enables the signal processing on a per-user basis in the iSCs, by providing the necessary level of flexibility and scalability. Besides, this architecture should also provide advantages in terms of throughput reduction of the signals transmitted over the backhauling link with respect to state of the art solutions. The throughput reduction is particularly important considering that broadband wireless communication systems (e.g. LTE/LTE-A and WiMAX) are capable of providing aggregate per-cell throughput in the order of hundreds of Mbps. Furthermore, a more efficient use of transmission resources between the RANaaS and the iSCs permits also to increase the maximum number of iSCs that can be connected to a given fibre ring.

Such new architecture should enable the signal processing on a per-user basis either within the iSCs or in a cooperative form involving multiple iSCs thanks to a particular partitioning of the baseband (L1) modem functionalities between the RANaaS and the iSCs. In particular, coding, HARQ, interleaving, modulation, MIMO processing and resource mapping are still performed in the RANaaS, while the per-user processing, IFFT, cyclic prefix insertion, filtering and RF conversion are performed in an enhanced iSC, as shown in Figure 4-10 for the transmitter part and Figure 4-11 for the receiver part. So, the signal transmitted over the optical fibre is the signal at the output/input of the resource mapping, where the user signals are separated in the frequency domain and the overall throughput with respect to the traditional RoF architecture is significantly reduced. The reduction comes from the fact that some ancillary information that just represents overhead (e.g. the cyclic prefix, the null subcarrier at the band edge) does not need to be transmitted over the fibre. A future activity in the framework of the project will be the calculation of the throughput reduction on the backhauling achievable by the FD-RoF architecture with respect to a conventional architecture.

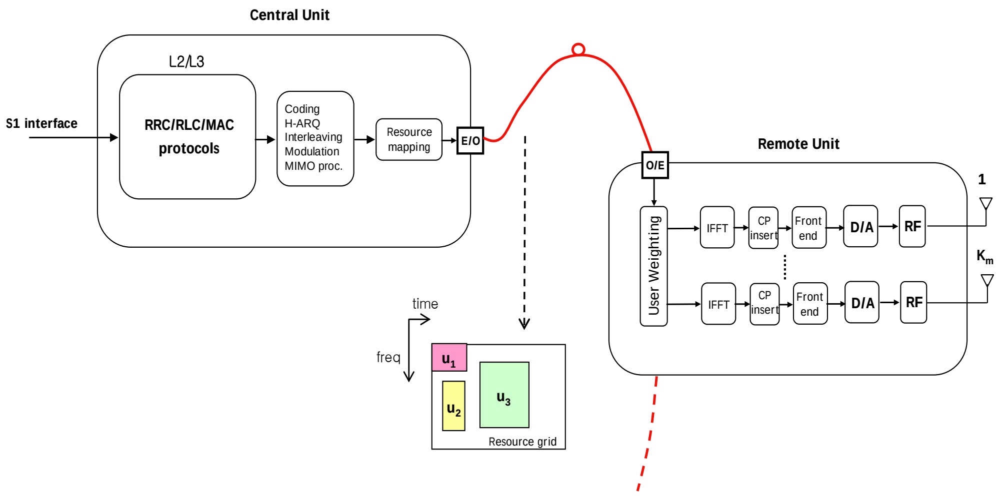

Figure 4-10: Frequency Domain RoF architecture: transmitter part

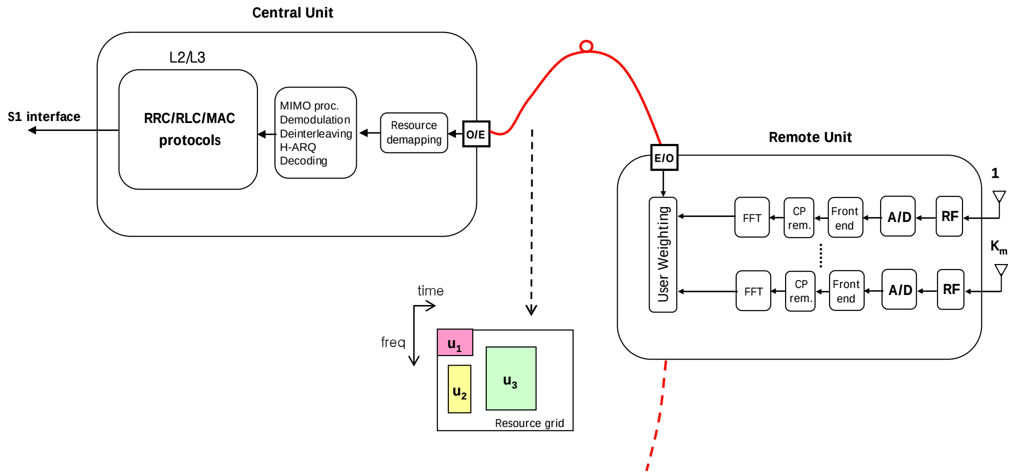

Figure 4-11: Frequency Domain RoF architecture: receiver part

As it can be easily seen, this novel architecture allows user-based signal processing operations such as adaptive beamforming or coordinated multipoint transmission to be performed in the iSC for each user separately while the calculation of the adaptive weighting coefficients can be performed either in the iSC or in the RANaaS if network coordination algorithms are required.

4.7.2 Assumptions

For the innovation concerning data transmission in FD mode the list of assumptions that are considered relevant is reported in Table 4-14. As for J1 and J2 interface, they are needed but the choice is left as optional because also traditional interfaces could co-exist with J1 and J2 and on the other hand it is not mandatory that all the iSCs are connected by J1 and J2. For wired and wireless assumption it is considered primarily the wired (i.e. fibre) option.

Table 4-14: Assumptions of CT2.6: Data compression over RoF

Assumption	Description	
A.1	Large number of iSCs in local area	x
A.2	Availability of macro BS in same frequency band (co-channel deployment)	o
A.3	Availability of macro BS in different frequency band	o
A.4	J1 interface between all iSCs and RANaaS with known parameters	*

A.5	J1 interface between some iSCs and RANaaS with known parameters	*
A.6	J2 interface for interconnections of all iSCs	*
A.7	J2 interface for interconnections of some iSCs (direct neighbours, selection)	*
A.8	Wired inter-node links between iSCs (fibre)	x
A.9	Wireless inter-node links between iSCs (60GHz)	*
A.10	Wired connection of iSCs to RANaaS (fibre)	x
A.11	Wireless connection of iSCs to RANaaS (60GHz)	*
A.12	Availability of a logical controller (iNC) for the joint RAN/BH optimization	o

4.7.3 Technology requirements

The list of requirements is reported in Table 4-15. In particular, it is stressed the requirement related to the capacity over J1 and J2 links, that is increased by this innovation. As for the requirement R.2.12 is deemed relevant only for the optional extension to the wireless case, to be evaluated in a later stage.

Table 4-15: Requirements of CT2.6: Date compression over RoF

Technical requirements	Description	
R.2.1	Limited capacity for J1 links (high, medium, low)	x
R.2.2	Limited capacity for J2 links (high, medium, low)	x
R.2.10	Access to the transceiver chain to implement FD approach in the transmission	x
R.2.11	Preferably fibre-based J1 and J2 interfaces	x
R.2.12	LOS between iSCs and RANaaS	x

4.7.4 iJOIN objectives addressed

The most relevant objectives that will be addressed are possibly the increase in area throughput and energy efficiency; on the other hand there could be the estimation of the cost efficiency reached by the adoption of this innovation.

4.8 CT2.7: 60GHz backhauling

4.8.1 Scenario description

The proposed scenario concerns the emerging technology of 60 GHz wireless links as a backhaul technology. As depicted in Figure 4-12, the scenario consists of two serial wireless links, the LTE radio access and a 60 GHz wireless link. A UE's signal is available as digital I/Q data in the iSC. The problem addressed in this candidate technology CT2.7 is to determine how much digital processing should take place in the iSC. Some PHY features like FEC might be reused in both links to reduce processing in the iSC, while too little processing increases the data load to be transmitted on the 60 GHz link. The goal of the investigation will be to determine an optimal functional split so that the throughput between UE and RANaaS can be maximized while the complexity in the iSC is kept as low as possible. This functional split should be flexible, as it might depend on variations in the traffic demand or the number of connected UEs. Principal investigation will be undertaken with one iSC and one UE, while later scenarios with multiple iSCs and UEs as well as multi-hop scenarios will be of interest.

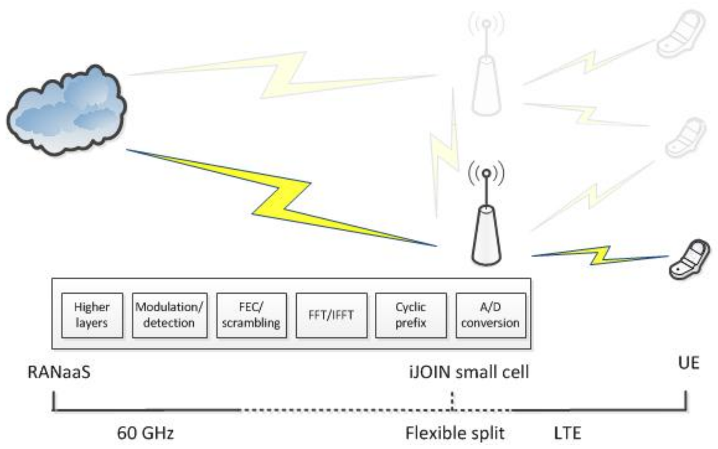

Figure 4-12: Scenario for 60 GHz backhauling

4.8.2 Assumptions

The preliminary set of assumptions for CT2.7 is summarized in Table 4-16.

Table 4-16: Assumptions of CT2.7: 60 GHz backhauling

Assumption	Description	
A.5	J1 interface between some iSCs and RANaaS with known parameters	x
A.9	Wireless inter-node links between iSCs (60GHz)	o
A.11	Wireless connection of iSCs to RANaaS (60GHz)	x
A.12	Availability of a logical controller (iNC) for the joint RAN/BH optimization	o
A.2.1	Global TxCSI at RANaaS	x
A.2.2	Local TxCSI at iSCs	x
A.2.3	Global RxCSI at RANaaS	x
A.2.4	Local RxCSI at iSCs	x
A.2.6	LTE Modulation & Coding Schemes	x
A.2.7	Gaussian Input Signals	x
A.2.9	Adaptive Coding and Modulation	o
A.2.10	Uplink Transmission	x
A.2.11	Downlink Transmission	x
A.2.13	Multiple Tx/Rx antennas at iSC	o

4.8.3 Technology requirements

The preliminary set of requirements for CT2.7 is summarized in Table 4-17.

Table 4-17: Requirements of CT2.7: 60 GHz backhauling

Technology requirements	Description	
R.2.1	Limited capacity for J1 links (high, medium, low)	x
R.2.2	Limited capacity for J2 links (high, medium, low)	o
R.2.3	Low latency for J1 links (zero, very small, small)	x

R.2.4	Low latency for J2 links (zero, very small, small)	o
R.2.7	Message exchange between iSCs and RANaaS (CPU) for partly distributed processing	x
R.2.8	Message forwarding of iSCs to RANaaS (CPU) for centralized processing	x
R.2.10	Access to the transceiver chain to implement FD approach in the transmission	x
R.2.12	LOS between iSC and RANaaS	x
R.2.13	Global TxCSI at RANaaS (CPU) (perfect, limited, imperfect)	o
R.2.14	Local TxCSI at iSCs (perfect, limited, imperfect)	o
R.2.15	Global RxCSI at RANaaS (CPU) (perfect, limited, imperfect)	o
R.2.16	Local RxCSI at iSCs (perfect, imperfect)	o
R.2.17	~2 GHz of BW on 60 GHz link	x

4.8.4 iJOIN objectives addressed

- Increase throughput and energy efficiency by optimizing the functional split.

5 Consolidated WP2 Assumptions

5.1 Architectural and technology deployment assumptions

The following table gives an overview over the architectural and technology deployment assumptions per CT and serves as a basis to derive the preliminary iJOIN architecture. The specific requirements will be investigated/derived based on this architecture.

Table 5-1: Architectural and deployment assumptions per Candidate Technology

Assumption	Description	2.1 UoB	2.2 SCBB	2.3 CEA	2.4 UNIS	2.5 IMC	2.6 TI	2.7 TUD
A.1	Large number of iSCs in local area	x	x		x	x	x	
A.2	Availability of macro BS in same frequency band (co-channel deployment)	o		*		o	o	
A.3	Availability of macro BS in different frequency band						o	
A.4	J1 interface between <u>all</u> iSCs and RANaaS with known parameters	o	x	*	x	x	*	
A.5	J1 interface between <u>some</u> iSCs and RANaaS with known parameters	x		x			*	x
A.6	J2 interface for interconnections of all iSCs	o	*		o	o	*	
A.7	J2 interface for interconnections of some iSCs (direct neighbours, selection)	x		x	o	x	*	
A.8	Wired inter-node links between iSCs (fibre)	*	*		o	*	x	
A.9	Wireless inter-node links between iSCs (60GHz)	*	*	x	o	*	*	o
A.10	Wired connection of iSCs to RANaaS (fibre)	*	*		o	*	x	
A.11	Wireless connection of iSCs to RANaaS (60GHz)	*	*	x	*		*	x
A.12	Availability of a logical controller (iNC) for the joint RAN/BH optimization	x	o		o	x	o	o

<u>Legend</u>

“x” mandatory assumption

“*“ optional choices for implementation candidates

“o” optional assumption; this not-mandatory feature may lead to improvements

“ “ not assumed for the CT

5.2 WP2 Implementation assumptions

The following table defines implementation assumptions per CT2.x describing the fundamental framework of the investigations. This list gives information about the operational mode for the investigations and what kind of information is required at the different places in the system.

Table 5-2: Implementation Assumptions per Candidate Technology

Assumption	Description	2.1 UoB	2.2 SCBB	2.3 CEA	2.4 UNIS	2.5 IMC	2.6 TI	2.7 TUD
A.2.1	Global TxCSI at RANaaS				x	o		x
A.2.2	Local TxCSI at iSCs			x	x	x		x
A.2.3	Global RxCSI at RANaaS		x			o		x
A.2.4	Local RxCSI at iSCs	x	x	x		x		x
A.2.5	Global RxCSI at iSCs					o		
A.2.6	LTE Modulation & Coding Schemes	x	x	*				x
A.2.7	Gaussian Input Signals				x	x		x
A.2.8	Perfect Channel Codes (infinite length)				x	x		
A.2.9	Adaptive Coding and Modulation			x				o
A.2.10	Uplink Transmission	x	x	x				x
A.2.11	Downlink Transmission				x			x
A.2.12	FDD / TDD				x			
A.2.13	Multiple Tx/Rx antennas at iSC	o	o		x	o		o

6 Summary and Conclusion

In this report, the general architecture for 3GPP LTE network is discussed. The SotA channel models for both the non-cooperative MIMO and cooperative systems are presented. The PHY parameters (e.g., modulation order, coding schemes) are also provided. Moreover, the discussion is provided for different performance indicators based on which different PHY techniques will be compared later on. The preliminary SotA PHY techniques are considered for the radio access network in order to improve the different performance indicators taking backhaul constraints into account. These techniques include: Distributed and iterative multiuser decoding, CoMP and ICIC, Joint network-channel coding and Frequency-domain RoF. Furthermore, various SotA backhaul types (Fibre-based, wireless and mmWave, and in-band using relay) are discussed and it is mentioned that each category has its own pros and cons.

Moreover, various CTs are described which utilize the aforementioned techniques for access network and backhauling in four different common scenarios. The common scenarios include: stadium, square, wide-area continuous coverage, indoor (airport/shopping mall). The assumptions and requirements of each CT are also explicitly mentioned. Finally, the consolidated assumptions and requirements for WP2 are presented. It is worth mentioning here that all the CTs discussed for the common scenarios have potential to achieve the iJOIN objectives.

Acknowledgements and Disclaimer

This work was partially funded by the European Commission within the 7th Framework Program in the context of the ICT project iJOIN (Grant Agreement No. 317941). The views and conclusions contained here are those of the authors and should not be interpreted as necessarily representing the official policies or endorsements, either expressed or implied, of the iJOIN project or the European Commission.

References

[1] Cisco Visual Networking Index: Global Mobile Data Traffic Forecast Update, 2012-2017, www.cisco.com, 2013

[2] 3GPP TS 36.101, "Radio Access Network; Evolved Universal Terrestrial Radio Access; (E-UTRA); User Equipment (UE) radio transmission and reception (Release 11), V11.3.0 (2012-12)

[3] REPORT ITU-R M.2134, "Requirements related to technical performance for IMT-Advanced radio interface(s)".

[4] 3GPP TR 36.814, "Further Advancements for E-UTRA Physical Layer Aspects (Release 9)". V9.0.0 (2010-03)

[5] 3GPP TR 25.913, "Requirements for Evolved UTRA (E-UTRA) and Evolved UTRAN (E-UTRAN) (Release 8)". V8.0.0 (2008-12)

[6] 3GPP TR 36.932, "Scenarios and Requirements for Small Cell Enhancements for E-UTRA and E-UTRAN (Release 12)". V12.0.0 (2012-12)

[7] Fahimeh Rezaei, "A Comprehensive Analysis of the LTE Physical Layer", University of Nebraska – Lincoln, [online: http://digitalcommons.unl.edu/ceendiss/8], 2010.

[8] 3GPP R1-082975, "Application scenarios for LTE-Advanced relay", RAN1 #54, China Mobile, Vodafone, Huawei, Aug 2008.

[9] ITU-R, ''Guidelines for evaluation of radio interface technologies for IMT-Advanced", Report ITU-R M.2135, Geneva, Switzerland, 2008.

[10] 3GPP R1-091566, "Relay to UE channel model for LTE-Advanced", RAN1 #56bis, CMCC, Mar 2009.

[11] 3GPP R1-100559, "Fast-fading modeling for outdoor Relay scenario", R1-100559, RAN1 #59bis, Valencia, Spain, Jan 2010.

[12] Y. Yuan, "LTE-A Relay Scenarios and Evaluation Methodology", in LTE-Advanced Relay Technology and Standardization, Signals and Communication Technology, Springer-Verlag 2013.

[13] 3GPP TR 25.996, "Spatial Channel Model for Multiple Input Multiple Output (MIMO) Simulations (Rel. 6)," Sept. 2003.

[14] P. Kyosti et al., "WINNER II Channel Models", IST-WINNER II D1.1.2, Nov. 2007.

[15] C. X. Wang et. al., "Cooperative MIMO channel models: A survey", *IEEE Communications Magazine*, vol. 48, no. 2, pp. 80-87, 2010.

[16] X. Cheng et. al., "Cooperative MIMO Channel Modeling and Multi-Link Spatial Correlation Properties", *IEEE Journal on Selected Areas in Communications*, vol. 30, no. 2, pp. 388-396, 2012.

[17] S. Khattak, W. Rave und G. Fettweis, "Distributed Iterative Multiuser Detection through Base Station Cooperation," EURASIP Journal on Wireless Communications and Networking, 2008.

[18] A. D. Wyner, "Shannon-theoretic approach to a Gaussian cellular multiple-access channel," IEEE Transactions on Information Theory, vol. 40, no. 6,, p. 1713–1727, 1994.

[19] A. Grant, S. Hanly, J. Evans und R. Müller, "Distributed decoding for Wyner cellular systems," in Proceedings of the 5th Australian Communications Theory Workshop (AusCTW '04), Newcastle, Australia, 2004.

[20] E. Aktas, J. Evans und S. Hanly, "Distributed decoding in a cellular multiple-access channel," in Proceedings of the IEEE International Symposium on Information Theory (ISIT '04), Chicago, USA, 2004.

[21] E. Aktas, J. Evans und S. Hanly, "Distributed base station processing in the uplink of cellular networks," in Proceedings of IEEE International Conference on Communications (ICC '06), Istanbul, Turkey, 2006.

[22] O. Shental, A. J. Weiss, N. Shental und Y. Weiss, “Generalized belief propagation receiver for near-optimal detection of twodimensional channels with memory,“ in Proceedings of the IEEE Information Theory Workshop (ITW '04), San Antonio, USA, 2004.

[23] A. Sklavos und T. Weber, “Interference suppression in multiuser OFDM systems by antenna diversity and joint detection,“ in Proceedings of the COST 273 Management Committee Meeting (MCM '01), Bologna, Italy, 2001.

[24] S. Khattak, W. Rave und G. Fettweis, “SIC based multiuser turbo detection in a distributed antenna system for non gray mapping,“ in Proceedings of the 9th International Symposium on Wireless Personal Multimedia Communications (WPMC '06), San Diego, USA, 2006.

[25] T. Mayer, H. Jenkac und J. Hagenauer, “Turbo Base-Station Cooperation for Intercell Interference Cancellation,“ in IEEE International Conference on Communications (ICC '06), Istanbul, Turkey, 2006.

[26] 3GPP, “TS 36.300: Evolved Universal Terrestrial Radio Access (E-UTRA) and Evolved Universal Terrestrial Radio Access Network (E-UTRAN); Overall description; Stage 2 (Release 11),” Nov. 2012

[27] C. Lanzani, G. Kardaras, and Deepak Boppana, “Remote Radio Heads and the Evolution Towards 4G Networks,” Altera Corporation White Paper, Feb. 2009, [online: mwww.altera.com/literature/wp/wp-01096-rrh-4g.pdf, accessed Feb. 2013]

[28] S. Sesia, I. Toufik and M. Baker, LTE - The UMTS Long Term Evolution: From Theory to Practice, John Wiley & Sons, 2009.

[29] A. Sendonaris, E. Erkip, and B. Aazhang, “User cooperation diversity. Part I. System description,” IEEE Transactions on Communications, vol. 51, no. 11, pp. 1927–1938, 2003.

[30] A. Sendonaris, E. Erkip, and B. Aazhang, “User cooperation diversity. Part II. Implementation aspects and performance analysis,” IEEE Transactions on Communications, vol. 51, no. 11, pp. 1939–1948, 2003.

[31] J.N. Laneman, D.N. Tse, and G.W. Wornell, “Cooperative diversity in wireless networks: efficient protocols and outage behaviour,” IEEE Trans. on Information Theory, vol. 50, no. 12, pp. 3062–3080, 2004.

[32] M. C. Valenti and B. Zhao, “Distributed turbo codes: towards the capacity of the relay channel,” in IEEE Vehicular Technology Conference (VTC), 2003, pp. 322–326.

[33] P. Razaghi and W. Yu, “Bilayer low-density parity-check codes for decode-and-forward in relay channels,” IEEE Trans. on Information Theory, vol. 53, no. 10, pp. 3723–3739, 2007.

[34] A. Chakrabarti, A. De Baynast, A. Sabharwal, and B. Aazhang, “Lowdensity parity-check codes for the relay channels,” IEEE Journal on Selected Areas in Communications, vol. 25, no. 2, pp. 280–291, 2007.

[35] J. Hu and T. M. Duman, “Low density parity check codes over wireless relay channels,” IEEE Trans. on Wireless Communications, vol. 6, no. 9, pp. 3384–3394, 2007.

[36] C. Li, G. Yue, M. A. Khojastepour, X. Wang, and M. Madihian, “LDPC coded cooperative relay systems: performance analysis and code design,” IEEE Trans. on Communications, vol. 56, no. 3, pp. 485–496, 2008.

[37] J. Cances and V. Meghdadi, “Optimized low density parity check codes designs for half duplex relay channels,” IEEE Trans. on Wireless Communications, vol. 8, no. 7, pp. 3390–3395, 2009.

[38] D. Duyck, J. J. Boutros, and M. Moeneclaey, “Low-density paritycheck coding for block fading relay channels,” in IEEE Inform. Theory Workshop (ITW), 2009, pp. 248–252.

[39] V. Savin, “Split-Extended LDPC codes for coded cooperation”, IEEE International Symposium on Information Theory and Applications (ISITA), Taichung, Taiwan, October 2010.

[40] R. Ahlswede, N. Cai, S.-Y. R. Li, and R. W. Yeung, “Network information flow,” IEEE Trans. Inform. Theory, vol. 46, no. 4, pp. 1204-1216, Jul. 2000.

[41] M. Di Renzo, L. Iwaza, M. Kieffer, P. Duhamel, K. Al-Agha, “Robust wireless network coding-an overview,” Lecture Notes of the Institute for Computer Sciences, Social Informatics and Telecommunications Engineering, 2010.

[42] Shengli Zhang, Yu Zhu, Soung-Chang Liew, and Khaled Ben Letaief, “Joint design of network coding and channel decoding for wireless networks,” in IEEE Wireless Communications and Networking Conference (WCNC), 2007, pp. 779–784.

[43] Dereje H Woldegebreal and Holger Karl, “Multiple-access relay channel with network coding and non-ideal source-relay channels,” in IEEE International Symposium on Wireless Communication Systems (ISWCS), 2007, pp. 732–736.

[44] Christoph Hausl, Joint network-channel coding for wireless relay networks, Ph.D. thesis, Technische Universitat Munchen, 2008.

[45] Tuan Tran, Thinh Nguyen, and Bella Bose, “A joint network-channel coding technique for single-hop wireless networks,” IEEE Workshop on Network Coding, Theory and Applications (NetCod), 2008, pp. 1–6.

[46] Christoph Hausl, “Joint network-channel coding for the multiple-access relay channel based on turbo codes,” European Transactions on Telecommunications, vol. 20, no. 2, pp. 175–181, 2009.

[47] Xiaoyan Xu, Mark F Flanagan, Norbert Goertz, and John Thompson, “Joint channel and network coding for cooperative diversity in a shared-relay environment,” IEEE Transactions on Wireless Communications, vol. 9, no. 8, pp. 2420–2423, 2010.

[48] Atoosa Hatefi, Raphael Visoz, and Antoine O Berthet, “Joint channel-network coding for the semi-orthogonal multiple access relay channel,” in IEEE Vehicular Technology Conference Fall (VTC-Fall), 2010, pp. 1–5.

[49] Peng Hui Tan, Chin Keong Ho, and Sumei Sun, “Joint network-channel code design for block fading cooperative multiple access channel,” in IEEE Information Theory Workshop (ITW), 2010, pp. 1–5.

[50] Jun Li, Jinhong Yuan, Robert Malaney, Marwan H Azmi, and Ming Xiao, “Network coded LDPC code design for a multi-source relaying system,” IEEE Transactions on Wireless Communications, vol. 10, no. 5, pp. 1538–1551, 2011.

[51] Zheng Guo, Jie Huang, Bing Wang, Shengli Zhou, Jun-Hong Cui, and Peter Willett, “A practical joint network-channel coding scheme for reliable communication in wireless networks,” IEEE Transactions on Wireless Communications, vol. 11, no. 6, pp. 2084–2094, 2012.

[52] Dieter Duyck, Daniele Capirone, Marc Moeneclaey, and Joseph J Boutros, “A full-diversity joint network-channel code construction for cooperative communications,” in IEEE Int. Symp. on Personal, Indoor and Mobile Radio Communications (PIMRC), 2009, pp. 1282–1286.

[53] Dieter Duyck, Daniele Capirone, Joseph J Boutros, and Marc Moeneclaey, “Analysis and construction of full-diversity joint network-LDPC codes for cooperative communications,” EURASIP Journal on Wireless Communications and Networking, vol. 2010, pp. 9, 2010.

[54] G. J. Foschini and M. J. Gans, “On limits of wireless communications in a fading environment when using multiple antennas,” Wireless Personal Communications, vol. 6, pp. 311–335, 1998

[55] E. T. Ar and I. E. Telatar, “Capacity of multi-antenna Gaussian channels,” European Transactions on Telecommunications, vol. 10, pp. 585–595, 1999.

[56] J. Lee and N. Jindal, “High SNR Analysis for MIMO Broadcast Channels: Dirty Paper Coding Versus Linear Precoding,” IEEE Trans. Inform. Theory, vol. 53, no.12, pp. 4787 – 4792, Dec. 2007.

[57] D. Gesbert, M. Kountouris, R. W. Heath, C-B. Chae and T. Salzer, “Shifting the MIMO Paradigm,” IEEE Sig. Process. Mag., vol. 24, no. 5, pp. 36 – 46, Sept. 2007.

[58] E. Pateromichelakis, M. Shariat, A. Quddus and R. Tafazolli, “On the evolution of multi-cell scheduling in 3GPP LTE/LTE-A,” IEEE Comm. Surveys & Tutorials, pp. 1-17 (early access).

[59] W. Choi, J. G. Andrews, “The capacity gain from intercell scheduling in multi-antenna systems,” IEEE Trans. Wireless Comm., vol. 7, no. 2, pp. 714-725, Feb. 2008.

[60] S. Shamai (Shitz) and B. M. Zaidel, “Enhancing the cellular downlink capacity via co-processing at the transmitting end,” in Proc. IEEE Veh. Technol. Conf., Rhodes, Greece, May 2001, pp. 1745–1749.

[61] H. Zhang and H. Dai, “Cochannel interference mitigation and cooperative processing in downlink multicell multiuser MIMO networks,” European J. Wireless Commun. and Networking, no. 2, pp. 222–235, 4th Quarter 2004.

[62] K. Karakayali, G. J. Foschini, R. A. Valenzuela, and R. Yates, “On the maximum common rate achievable in a coordinated network,” in Proc. IEEE Int. Conf. Commun., Istanbul, Turkey, June 2006, pp. 4333–4338.

[63] G. J. Foschini, H. Huang, K. Karakayali, R. A. Valenzuela, and S. Venkatesan, “The value of coherent base station coordination,” in Proc., Conference on Information Sciences and Systems (CISS), Johns Hopkins University, Mar. 2005.

[64] O. Somekh, O. Simeone, Y. Bar-Ness, and A. M. Haimovich, “Distributed multi-cell zero-forcing beamforming in cellular downlink channels,” in Proc. IEEE Globecom, San Francisco, Nov. 2006, pp. 1–6.

[65] J. Zhang, R. Chen, J. G. Andrews, A. Ghosh and R.W. Heath, “Networked MIMO with clustered linear precoding,” IEEE Trans. Wireless Comm., vol. 8, no. 4, April 2009.

[66] J. Zhang and J. G. Andrews, “Adaptive spatial intercell interference cancellation in multicell wireless networks,” in IEEE Jour. Sel. Areas Comm., vol. 28, no. 9, Dec. 2010.

[67] H. Dahrouj and W. Yu, “Coordinated beamforming for the multicell multi-antenna wireless system,” in IEEE Trans. Wireless Comm., vol. 9, no. 5, May 2010.

[68] P. Marsch and G. Fettweis, “On downlink network MIMO under a constrained backhaul and imperfect channel knowledge,” in Proc. IEEE GlobeCom, 2009.

[69] R. Zakhour and D. Gesbert, “Optimized data sharing in multicell MIMO with finite backhaul capacity,” IEEE Trans. Sig. Process., vol. 59, no.12, pp. 6102-6111, Dec. 2011.

[70] N. Seifi, M. Viberg, R. W. Heath, J. Zhang, and M. Coldrey, “Coordinated single-cell vs multi-cell transmission with limited-capacity backhaul,” in Proc. IEEE ACSSC, 2010.

[71] Q. Zhang, C. Yang and A. F. Molisch, “Cooperative downlink transmission mode selection under limited-capacity backhaul,” in Proc. Wireless Communications and Networking Conference (WCNC), Apr. 2012, pp. 1082 – 1087.

[72] Common Pubblic Radio Interface - http://www.cpri.info/

[73] Open Base Station Architecture Initiative - http://www.obsai.com/

[74] 3GPP TS 36.211, “Radio Access Network; Evolved Universal Terrestrial Radio Access; (E-UTRA); Physical channels and modulation”, Release 10, (2012 - 12).

[75] J. Segel, M. Weldon, LightRadio Portfolio: Technical Overview, Alcatel Lucent Technology White Paper, 2011, http://www.alcatel-lucent.com

[76] NGMN White Paper on LTE Backhauling deployment scenarios, http://www.ngmn.org/uploads/media/NGMN_Whitepaper_LTE_Backhauling_Deployment_Scenarios_01.pdf

[77] Ceragon, “Wireless Backhaul Solutions for Small Cells”, Solution Brief, available online: http://www.ceragon.com/files/library/Ceragon_Small_Cell-Solution_Brief.pdf, accessed Feb. 2013.

[78] Wells, J.; , "Faster than fiber: The future of multi-G/s wireless," *Microwave Magazine*, *IEEE* , vol.10, no.3, pp.104-112, May 2009.

[79] Z. Pi and f. Khan, “An introduction to millimetre-wave mobile broadband systems”, IEEE Comm. Mag., pg. 101-107, June 2011.

[80] 3GPP TS 36.212, “Radio Access Network; Evolved Universal Terrestrial Radio Access; (E-UTRA); Multiplexing and channel coding”, Release 10, (2012 - 12).

[81] Rohde & Schwarz, "UMTS Long Term Evolution (LTE) Technology Introduction", Application Note 1MA111, 2008.

[82] ETSI, ''Open Radio Equipment Interface (ORI); Requirements for Open Radio equipment interface (ORI)", Release 1, ETSI GS ORI 001 V1.2.1 (2012 - 08). [online: http://www.etsi.org/deliver/etsi_gs/ORI/001_099/001/01.02.01_60/gs_ORI001v010201p.pdf, accessed April. 2013]

[83] ETSI TR 101 112: "Selection procedures for the choice of radio transmission technologies of the UMTS", UMTS 30.03 version 3.1.0.

